

Fly stage trypanosomes recycle glucose catabolites and TCA cycle intermediates to stimulate growth in near physiological conditions

Oriana Villafraz¹, Marc Biran², Erika Pineda¹, Nicolas Plazolles¹, Edern Cahoreau^{3,4}, Rodolpho Ornitz Oliveira Souza⁵, Magali Thonnus¹, Stefan Allmann⁶, Emmanuel Tetaud¹, Loïc Rivière¹, Ariel M. Silber⁵, Michael P. Barrett^{7,8}, Alena Zíková⁹, Michael Boshart⁶, Jean-Charles Portais^{3,4,10}, Frédéric Bringaud^{1,#}

¹ Univ. Bordeaux, CNRS, Microbiologie Fondamentale et Pathogénicité (MFP), UMR 5234, F-33000 Bordeaux, France

² Univ. Bordeaux, CNRS, Centre de Résonance Magnétique des Systèmes Biologiques (CRMSB), UMR 5536, F-33000 Bordeaux, France

³ Toulouse Biotechnology Institute, TBI-INSA de Toulouse INSA / CNRS 5504-UMR INSA/INRA 792, Toulouse, France

⁴ MetaToul-MetaboHub, National Infrastructure of Metabolomics and Fluxomics, Toulouse, 31077, France

⁵ Laboratory of Biochemistry of Tryps - LaBTryps, Department of Parasitology, Institute of Biomedical Sciences, University of São Paulo, São Paulo, Brazil

⁶ Fakultät für Biologie, Genetik, Ludwig-Maximilians-Universität München, Grosshadernerstrasse 2-4, D-82152 Martinsried, Germany

⁷ Wellcome Centre for Integrative Parasitology, Institute of Infection, Immunity and Inflammation, College of Medical, Veterinary and Life Sciences, University of Glasgow, Glasgow, United Kingdom

⁸ Glasgow Polyomics, Wolfson Wohl Cancer Research Centre, Garscube Campus, College of Medical Veterinary and Life Sciences, University of Glasgow, Glasgow, United Kingdom

⁹ Institute of Parasitology, Biology Center, Czech Academy of Sciences and Faculty of Science, University of South Bohemia, České Budějovice 370 05, Czech Republic

¹⁰ RESTORE, Université de Toulouse, CNRS ERL5311, EFS, ENVT, Inserm U1031, UPS, Toulouse, France

Short title: A full TCA cycle operates in procyclic trypanosomes

Key words: *Trypanosoma brucei*; procyclic and epimastigote forms; carbon source (re-)used; mitochondrial metabolism; organellar redox balance; α -ketoglutarate toxicity; TCA cycle functionality

*Corresponding author: frederic.bringaud@u-bordeaux.fr

40 **Author Summary**

41 In the midgut of its insect vector, trypanosomes rely on proline to feed their energy metabolism.
42 However, the availability of other potential carbon sources that can be used by the parasite is
43 currently unknown. Here we show that tricarboxylic acid (TCA) cycle intermediates, *i.e.*
44 succinate, malate and α -ketoglutarate, stimulate growth of procyclic trypanosomes incubated in
45 medium containing 2 mM proline, which is in the range of the amounts measured in the midgut
46 of the fly. Some of these additional carbon sources are needed for the development of
47 epimastigotes, which differentiate from procyclics in the midgut of the fly, since their growth
48 defect observed in the presence of 2 mM proline is rescued by addition of α -ketoglutarate. In
49 addition, we have implemented new approaches to study a poorly explored branch of the TCA
50 cycle converting malate to α -ketoglutarate, which was previously described as non-functional in
51 the parasite, regardless of the glucose levels available. The discovery of this branch reveals that a
52 full TCA cycle can operate in procyclic trypanosomes. Our data broaden the metabolic potential
53 of trypanosomes and pave the way for a better understanding of the parasite's metabolism in
54 various organ systems of the tsetse fly, where it evolves.

55

56 **Abstract** (300 words)

57 *Trypanosoma brucei*, a protist responsible for human African trypanosomiasis (sleeping
58 sickness), is transmitted by the tsetse fly, where the procyclic forms of the parasite develop in the
59 proline-rich (1-2 mM) and glucose-depleted digestive tract. Proline is essential for the midgut
60 colonization of the parasite in the insect vector, however other carbon sources could be available
61 and used to feed its central metabolism. Here we show that procyclic trypanosomes can consume
62 and metabolize metabolic intermediates, including those excreted from glucose catabolism
63 (succinate, alanine and pyruvate), with the exception of acetate, which is the ultimate end-
64 product excreted by the parasite. Among the tested metabolites, tricarboxylic acid (TCA) cycle
65 intermediates (succinate, malate and α -ketoglutarate) stimulated growth of the parasite in the
66 presence of 2 mM proline. The pathways used for their metabolism were mapped by proton-
67 NMR metabolic profiling and phenotypic analyses of a dozen RNAi and/or null mutants
68 affecting central carbon metabolism. We showed that (i) malate is converted to succinate by both
69 the reducing and oxidative branches of the TCA cycle, which demonstrates that procyclic
70 trypanosomes can use the full TCA cycle, (ii) the enormous rate of α -ketoglutarate consumption
71 (15-times higher than glucose) is possible thanks to the balanced production and consumption of
72 NADH at the substrate level and (iii) α -ketoglutarate is toxic for trypanosomes if not
73 appropriately metabolized as observed for an α -ketoglutarate dehydrogenase null mutant. In
74 addition, epimastigotes produced from procyclics upon overexpression of RBP6, showed a
75 growth defect in the presence of 2 mM proline, which is rescued by α -ketoglutarate, suggesting
76 that physiological amounts of proline are not sufficient *per se* for the development of
77 trypanosomes in the fly. In conclusion, these data show that trypanosomes can metabolize
78 multiple metabolites, in addition to proline, which allows them to confront challenging
79 environments in the fly.

80

81 Introduction

82 *Trypanosoma brucei* is a hemoparasitic unicellular eukaryote sub-species of which cause Human
83 African Trypanosomiasis (HAT), also known as sleeping sickness. The disease, fatal if
84 untreated, is endemic in 36 countries in sub-Saharan Africa, with about 70 million people living
85 at risk of infection [1]. The *T. brucei* life cycle is complex and the parasite must adapt to several
86 dynamic environments encountered both in the insect vector, tsetse fly, and in the mammalian
87 hosts. This is accomplished by cellular development, including adaptations of energy
88 metabolism. Here, we focus on the insect stages of the parasite, the midgut procyclic (PCF) and
89 epimastigote forms, by providing a comprehensive analysis of the carbon sources capable of
90 feeding its central metabolism in tissue culture.

91 In glucose-rich mammalian blood, the metabolism of *T. brucei* bloodstream forms (BSF) relies
92 on glucose, with most of the glycolytic pathway occurring in specialized peroxisomes called
93 glycosomes [2]. BSF convert glucose, their primary carbon source, to the excreted end-product
94 pyruvate, although low but significant amounts of acetate, succinate and alanine are also
95 produced [3,4]. In contrast, the PCF mainly converts glucose to excreted acetate and succinate,
96 in addition to smaller amounts of alanine, pyruvate and lactate [5]. Although PCF trypanosomes
97 prefer to use glucose to support their central carbon metabolism *in vitro* [6,7], they rely on
98 proline metabolism in the fly midgut [8]. This is due to the presumed low abundance, or absence,
99 of free glucose in the hemolymph and tissues of the insect vector, which rely on amino acid for
100 their own energy metabolism [9]. In this particular *in vivo* context, the PCF has developed an
101 energy metabolism based on proline, which is converted to alanine, succinate and acetate (see
102 Fig 1A) [7,10].

103 As in other organisms, *T. brucei* PCF catabolism of proline is achieved by oxidation to
104 glutamate, through proline dehydrogenase (PRODH, step 1 in Fig 1) [6] and pyrroline-5
105 carboxylate dehydrogenase (P5CDH, step 3) [8]. RNAi-mediated downregulation of *P5CDH*
106 expression (^{RNAi}P5CDH) is lethal for the PCF grown in glucose-depleted medium containing 6
107 mM proline (glucose-depleted conditions) and abolishes fly infections. This demonstrated that
108 proline is essential for growth and development of insect-stage trypanosomes *in vivo* [8]. Proline
109 derived glutamate is then converted, by alanine aminotransferase (AAT, step 4), to the TCA
110 cycle intermediate α -ketoglutarate [11], which is further metabolized to succinate (steps 5-6) and
111 malate (steps 7 and 10) *via* the TCA cycle enzymes working in the oxidative direction [7].

112 Alternatively, glutamate dehydrogenase, which catalyzes an oxidative deamination of glutamate,
113 could also be involved in the production of α -ketoglutarate, as proposed for *T. cruzi*, but this has

114 never been demonstrated in *T. brucei* [12]. Malate is then converted to pyruvate by the malic
115 enzymes (step 15) [13], and serves as a substrate, together with glutamate, for AAT to produce
116 α -ketoglutarate and secreted alanine (step 4). Alternatively, pyruvate is converted by the
117 pyruvate dehydrogenase complex (PDH, step 16) to acetyl-CoA, which is further metabolized
118 into the excreted end-product acetate by two redundant enzymes, *i.e.* acetyl-CoA thioesterase
119 (ACH, step 17) and acetate:succinate CoA-transferase (ASCT, step 18) [14]. It is noteworthy
120 that oxidation of acetyl-CoA through the TCA cycle (dashed lanes in Fig 1A), initiated by
121 production of citrate by citrate synthase (CS, step 12), has not been detected so far in *T. brucei*
122 [15]. Consequently, it is currently considered that the TCA cycle does not work as a cycle in
123 trypanosomes, which only use branches of the TCA cycle fed by anaplerotic reactions [16].
124

125 **Fig 1. Proline metabolism of the PCF trypanosomes in the presence of other carbon**
126 **sources.** Panels A, B, C and D correspond to schematic metabolic representations of PCF
127 trypanosomes incubated in glucose-depleted medium, containing proline (grey arrows) without
128 or with succinate (red arrows), malate (green arrows) and α -ketoglutarate (blue arrows),
129 respectively. End-products excreted from catabolism of proline and the other carbon sources are
130 shown in rectangles with the corresponding colour code and the enzyme numbers under
131 investigation are circled. Enzymatic reactions of proline metabolism that have not been shown to
132 occur in parental PCF are represented by dashed lines. Similarly, the red (A) and blue (D) dashed
133 arrows highlight that these reactions have not been formally demonstrated to occur in the
134 catabolism of succinate and α -ketoglutarate, respectively. In panel C, enzymatic reactions
135 occurring in the reducing direction of the TCA cycle are shown in light green. The production
136 and consumption of ATP and NAD⁺ are indicated in bold and the asterisks mean that production
137 of 2-hydroxyglutarate from proline has not been previously described for PCF. It should be noted
138 that, according to the literature, the TCA cycle does not work as a cycle in trypanosomes and
139 only branches are used through anaplerotic reactions [16]. Indicated enzymes are : 1, proline
140 dehydrogenase (PRODH); 2, spontaneous reaction; 3, pyrroline-5 carboxylate dehydrogenase
141 (P5CDH); 4, alanine aminotransferase (AAT); 5, α -ketoglutarate dehydrogenase complex
142 (KDH); 6, succinyl-CoA synthetase (SCoAS); 7, succinate dehydrogenase (SDH, complex II of
143 the respiratory chain); 8, respiratory chain and mitochondrial ATP synthetase (oxidative
144 phosphorylation); 9, mitochondrial NADH-dependent fumarate reductase (FRDm1); 10,
145 mitochondrial fumarase (FHm); 11, mitochondrial malate dehydrogenase (MDHm); 12, citrate
146 synthase (CS); 13, aconitase (ACO); 14, mitochondrial isocitrate dehydrogenase (IDHm); 15,

147 mitochondrial malic enzyme (MEM); 16, pyruvate dehydrogenase complex (PDH); 17, acetyl-
148 CoA thioesterase (ACH); 18, acetate:succinate CoA-transferase (ASCT); 19, unknown enzyme;
149 20, possibly NADH-dependent glutamate dehydrogenase.

150
151 The essential role of proline metabolism to trypanosomes in the insect vector has been well
152 established [8]. However, the utilization of other carbon sources that may be available in the
153 digestive tract and other organs of the insect, as well as the pathways of central carbon
154 metabolism used by trypanosomes *in vivo*, are currently unknown or poorly understood. For
155 instance, the transient availability of glucose for trypanosomes directly following tsetse blood
156 meals could contribute significantly to parasite development in the midgut of the fly. In addition,
157 possible metabolic interactions between trypanosomes and intestinal symbiotic bacteria might
158 also be taken into account, as illustrated by the positive correlation between the presence of
159 facultative symbionts including *Wigglesworthia glossinidia* and *Sodalis glossinidius* and the
160 ability of the tsetse fly to be infected by *T. brucei* [17,18]. Indeed these bacteria have been
161 proposed to create a metabolic symbiosis with *T. brucei* through provision of precursors to
162 threonine biosynthesis [19].

163 Here we show that PCF metabolizes carbon sources other than glucose and proline, such as
164 succinate, alanine, pyruvate, malate and α -ketoglutarate. Interestingly, the TCA cycle
165 intermediates succinate, malate and α -ketoglutarate stimulate growth of the parasites in *in vivo*-
166 like conditions (2 mM proline [20], without glucose). We also took advantage of the high
167 metabolic rate of these TCA cycle intermediates, to study the metabolic capacity of the parasite.
168 This approach provided the first evidence for a complete canonical TCA cycle in PCF
169 trypanosomes.

170

171 **Results**

172 **Procyclic trypanosomes can re-metabolize end-products excreted from glucose degradation**

173 To study the capacity of trypanosomes to metabolize unexpected carbon sources, such as those
174 possibly excreted from the metabolism of the fly microbiota, we developed a model in which
175 procyclic trypanosomes (PCF) have the possibility to re-consume partially oxidized metabolites
176 excreted from their own glucose catabolism. It is noteworthy that this model may also represent
177 an *in vivo* situation, when established PCF are exposed to a new blood meal of the insect. In this
178 experimental model, the parasites were incubated at a high density in PBS containing low
179 amounts of ^{13}C -enriched glucose ([U- ^{13}C]-glucose, 0.5 mM) in the presence or absence of 4 mM

180 proline. The production and possible re-consumption of excreted end-products from the
181 metabolism of [U-¹³C]-glucose and/or non-enriched proline was monitored by analyzing the
182 medium over-time during a 6 h incubation period using the ¹H-NMR profiling approach. This
183 quantitative ¹H-NMR approach was previously developed to distinguish between [¹³C]-enriched
184 and non-enriched excreted molecules produced from [¹³C]-enriched and non-enriched carbon
185 sources, respectively [21–23]. In these conditions, all glucose is consumed within the first 1.5-2
186 h (Fig 2A-B). When [U-¹³C]-glucose is the only carbon source, PCF convert it to ¹³C-enriched
187 acetate, succinate, alanine and pyruvate, in addition to lower amounts of non-enriched
188 metabolites produced from an unknown internal carbon source (ICS) [21–23]. After 1 h of
189 incubation, net production of ¹³C-enriched succinate and pyruvate stopped while glucose
190 remained in the medium. Interestingly, ¹³C-enriched acetate was still excreted even after glucose
191 depletion, suggesting that acetate was produced from the metabolism of excreted end-products,
192 such as succinate and pyruvate (Fig 2A, top). The same pattern was observed from the non-
193 enriched excreted metabolites produced from the ICS (Fig 2A, low).

194 Addition of proline strongly stimulated this re-utilization of glucose-derived succinate (Fig 2B,
195 top). In these incubation conditions, glucose-derived pyruvate was no longer excreted since it is
196 used as a substrate by alanine aminotransferase (AAT, step 4 in Fig 1A) to convert proline-
197 derived glutamate to α -ketoglutarate [7]. Alanine was also re-used, although with a 2.5 h delay
198 compared to succinate. This re-utilization was also seen for proline-derived succinate (Fig 2B,
199 low) as proline-derived acetate increased at the expense of succinate after 4.5 h of incubation.
200 Combined, these data suggested that glucose-derived and/or proline-derived succinate, pyruvate
201 and to a lower extent alanine can be re-utilized and converted to acetate.

202 Since acetate is produced by both the acetate:succinate CoA-transferase (ASCT, step 18 in Fig
203 1A) and the acetyl-CoA thioesterase (ACH, step17), the role of the acetate branch in the further
204 metabolism of excreted end-products was addressed. The same time-course was conducted on a
205 $\Delta ach/^{RNAi}$ ASCT double mutant, in which ASCT expression was knocked down by RNAi in the
206 null ACH background. After 2 days of incubation, the tetracycline induced $\Delta ach/^{RNAi}$ ASCT
207 ($\Delta ach/^{RNAi}$ ASCT.i) cell line showed an 80% reduction in acetate production from glucose
208 metabolism, compared to the parental cell line (Fig 2B-C), which is consistent with the 90%
209 reduction in acetate excretion previously described for this cell line [21]. The residual acetate
210 production was attributed to incomplete downregulation of ASCT expression, although ASCT
211 could not be detected by Western blot [21] (Fig 2C). The excretion of glucose-derived pyruvate
212 in the $\Delta ach/^{RNAi}$ ASCT.i mutant relates to the limited capacity of the acetate branch. Interestingly,

213 succinate and pyruvate excreted during the first hour of incubation are re-consumed and
214 converted to acetate and alanine, indicating that alanine is the ultimate excreted end-product
215 when the acetate branch is limiting (Fig 2C).

216
217 **Fig 2. Kinetic analyses of end-products excretion from [U-¹³C]-glucose and proline**
218 **metabolism.** PCF cells were incubated for 6 h in PBS containing 0.5 mM [U-¹³C]-glucose in the
219 presence (panel B) or not (panel A) of 4 mM non-enriched proline (Pro). Excreted end-products
220 were analyzed in the spent medium every 0.5 h by ¹H-NMR spectrometry. The top panels A and
221 B show the amounts of ¹³C-enriched end-products excreted from [U-¹³C]-glucose metabolism
222 and the amounts of glucose present in the spent medium. The bottom panels show the amounts
223 of non-enriched end-products produced from the metabolism of the unknown internal carbon
224 source (panel A) or from the metabolism of proline plus the unknown internal carbon source
225 (panel B). In panel C, the kinetics of end-products excreted from 0.5 mM [U-¹³C]-glucose in the
226 presence of 4 mM proline was determined for the Δach^{RNAi} ASCT.i mutant cell line as performed
227 in panel B. Western blot controls with the anti-ASCT and anti-aldolase immune sera are shown
228 below the graph.

229
230 **Succinate, pyruvate and alanine are metabolized in the presence of glucose or proline**
231 To determine how the main end-products excreted from glucose catabolism (succinate, alanine,
232 pyruvate or acetate) are metabolized in the presence or absence of glucose or proline, we
233 analyzed, by quantitative ¹H-NMR, the exometabolome of PCF incubated with [U-¹³C]-
234 succinate, [U-¹³C]-alanine, [U-¹³C]-pyruvate or [U-¹³C]-acetate in the presence or absence of
235 equal amounts of non-enriched glucose or proline. Succinate was poorly consumed alone,
236 however, the presence of glucose or proline stimulates its consumption by 3.6- and 4.6-fold,
237 respectively (Fig 3A). This is consistent with the increased conversion of glucose-derived
238 succinate to acetate, in the presence of proline (Fig 2A-B). The quantities of excreted end-
239 products from proline catabolism were reduced only 8% in the presence of succinate, compared
240 to a 53% reduction in the presence of glucose (Fig 3A). This suggests that, in contrast to the
241 previously reported glucose-induced downregulation of proline metabolism [6,7], succinate
242 addition does not limit the rate of proline metabolism. In the presence of [U-¹³C]-proline,
243 succinate is converted to malate, acetate, alanine and traces of fumarate, which represent 40.5%,
244 43.2%, 16.4% and 1.5% of the excreted end-products, respectively (Fig 3B). According to the
245 current metabolic model, succinate enters the tricarboxylic acid (TCA) cycle where it is
246 converted to fumarate by succinate dehydrogenase (SDH, step 7 in Fig 1B) and to malate by the

247 mitochondrial fumarase (FHM, step 10). The malic enzymes then produce pyruvate (MEM, step
248 15 and the cytosolic MEc not shown), which feeds the AAT (step 4) for production of alanine, or
249 the pyruvate dehydrogenase (PDH) complex plus the ACH/ASCT steps (steps 17 and 18) for
250 production of acetate. In agreement with this model, extracellular succinate and proline-derived
251 succinate were no longer metabolized to acetate in the ^{RNAi}SDH.i cell line (Fig 3B). As expected,
252 acetate production from succinate, as well as from proline, was abolished in the tetracycline-
253 induced PDH subunit E2 RNAi mutant cell line (^{RNAi}PDH-E2.i). The effective block of PDH
254 activity is reflected by the increased excretion of succinate-derived pyruvate, the substrate of the
255 PDH complex (Fig 3B).

256 [U-¹³C]-Alanine was poorly metabolized alone, but addition of glucose or proline considerably
257 stimulated its consumption, with the production of ¹³C-enriched end-products being 23-fold and
258 10-fold increased, respectively (Fig 3A). ¹³C-enriched acetate represents 100% and 82% of the
259 excreted end-products from [U-¹³C]-Alanine in the presence of proline and glucose, respectively
260 (S1 Table). [U-¹³C]-Pyruvate was converted to ¹³C-enriched alanine and acetate in the presence
261 or absence of glucose or proline. The rate of end-product excretion was only increased by 35%
262 and 17% in the presence of glucose and proline, respectively (Fig 3A). In contrast, no ¹³C-
263 enriched molecules were detected by ¹H-NMR in the exometabolome of PCF incubated with [U-
264 ¹³C]-acetate, in the presence or absence of glucose or proline, suggesting that acetate is not
265 further metabolized through the central metabolism (Fig 3A). Together, these data show that
266 acetate is the ultimate excreted end-product of the metabolism of glucose and other carbon
267 sources, while succinate, pyruvate and alanine, which are also excreted, can be re-utilized and
268 converted to acetate.

269
270 **Fig 3. Proton (¹H) NMR analyses of end-products excreted from the metabolism of ¹³C-**
271 **enriched succinate, alanine, pyruvate and acetate.** In panel A, PCF trypanosomes were
272 incubated for 6 h in PBS containing 4 mM [U-¹³C]-succinate, [U-¹³C]-alanine, [U-¹³C]-pyruvate
273 or [U-¹³C]-acetate alone or in combination with 4 mM glucose (+Glc) or proline (+Pro) before
274 analysis of the spent medium by ¹H-NMR spectrometry. As reference, the same experiment was
275 performed with 4 mM proline (Pro), 4 mM glucose (Glc) or 4 mM glucose with 4 mM [U-¹³C]-
276 proline (¹³C-Pro). The amounts of each end-product excreted are documented in S1 Table. Panel
277 B shows equivalent ¹H-NMR spectrometry experiments performed on the parental (WT),
278 ^{RNAi}SDH.i, ^{RNAi}PDH-E2.i and $\Delta kdh-e2$ cell lines incubated with 4 mM [U-¹³C]-proline and 4 mM
279 succinate. Because of high background, ¹³C-enriched 2-hydroxyglutarate produced from [U-¹³C]-
280 proline cannot be quantified, however, it is detectable in the $\Delta kdh-e2$ cell line as indicated by an

281 asterisk (*). Traces of fumarate produced from these carbon sources are not shown in the figure.
282 Abbreviations: A, acetate; Al, alanine; H, 2-hydroxyglutarate; K, α -ketoglutarate; M, malate; P,
283 pyruvate; S, succinate; nd, not detectable; *, detectable but not quantifiable. The efficiency of
284 RNAi-mediated downregulation of SDH and PDH-E2 expression in the tetracycline-induced (.i)
285 or non induced (.ni) cell line, as well as in the parental cell line (WT), was determined by SDH
286 activity assays (panel C) and Western blotting with the anti-PDH-E2 and anti-enolase (control)
287 immune sera (panel D). Panel E shows a PCR analysis of genomic DNA isolated from the
288 parental (WT) and $\Delta kdh-e2$ cell line. Lanes 1 to 6 of the gel picture correspond to different PCR
289 products described in the right panel. As expected, PCR amplification of the *KDH-E2* gene
290 (lanes 1-2) was only observed in the parental cell line, while *PAC* and *BSD* PCR-products were
291 observed only in the $\Delta kdh-e2$ mutant (lanes 3-4 and 5-6, respectively).

292
293 **TCA cycle intermediates stimulate growth of the PCF in *in vivo*-like conditions**
294 The midgut of the tsetse fly, the natural environment of PCF, lacks glucose between blood meals
295 and contains proline in the low mM range (1-2 mM) [20], which is used by the parasite for its
296 energy metabolism [8]. To determine if succinate, alanine, acetate, pyruvate and lactate stimulate
297 growth of the parasite in insect-like conditions, we estimated the growth of the PCF
298 trypanosomes as a function of increasing concentrations of these metabolites in the glucose-
299 depleted SDM79 medium containing 2 mM proline, using the Alamar Blue assay, as previously
300 described [23]. Among them, succinate (1 to 10 mM) was able to stimulate growth, with a
301 maximum effect at 10 mM, while pyruvate showed a moderate effect (S1 Fig). This succinate-
302 dependent growth stimulation is observed in the presence of up to 2 mM proline, but not in high-
303 proline conditions (12 mM) (Fig 4A). As controls, 1 to 20 mM proline stimulated growth in the
304 presence 0.2 mM and 2 mM proline, but not in the presence of 12 mM proline. Among six other
305 TCA cycle intermediates tested plus glutamate and aspartate, malate and α -ketoglutarate also
306 stimulated growth in the presence of 2 mM proline (and 0.2 mM), with a maximum effect on
307 growth also at 10 mM (S1 Fig and Fig 4A). This growth stimulation was confirmed by
308 performing growth curves on cells maintained in the exponential growth phase (between 10^6 and
309 10^7 cells/ml) over 15 days in the presence of 2 mM proline and 10 mM of succinate, malate or α -
310 ketoglutarate (Fig 4B). In the presence of these metabolites the culture doubling time was
311 reduced by approximately 1.2 fold, with an increased growth rate compared to that using 2 mM
312 proline alone. As observed for succinate, NMR analyses of excreted end-products from the
313 metabolism of malate and α -ketoglutarate showed that the addition of equimolar amounts of [U-

314 ^{13}C]-proline induced an increase of the rate of malate and α -ketoglutarate consumption by 5.7
315 and 6.6 fold, respectively (Fig 4C). 6.9 and 2.8 fold increases of malate and α -ketoglutarate
316 consumption were seen with $[\text{U-}^{13}\text{C}]$ -glucose, respectively.

317 The effect of succinate, malate and α -ketoglutarate was also determined on PCF grown in
318 glucose-rich conditions. At most, succinate, α -ketoglutarate and the proline control have a minor
319 stimulatory effect in the presence of 2 mM or 12 mM glucose (2 mM proline) (Figs 4A-B).
320 However, addition of 10 mM malate to PCF grown in the presence 2 mM glucose slightly
321 slowed growth of the parasite (Fig 4B). Malate was consumed 22% more in glucose-rich than in
322 glucose-depleted conditions and its presence induced a 27% reduction of glucose consumption
323 (Fig 4C), suggesting that switch to partial malate metabolism is less efficient than catabolism of
324 glucose alone.

325
326 **Fig 4. Succinate, malate and α -ketoglutarate stimulate growth of the PCF.** Panel A shows
327 growth of the PCF trypanosomes in the glucose-depleted SDM79 medium containing 0.2 mM, 2
328 mM (low-proline) or 12 mM (high-proline) proline, 2 mM glucose/2 mM proline (low-glucose)
329 or 12 mM glucose/2 mM proline (high-glucose) in the presence of added 10 μM to 100 mM
330 succinate, malate, α -ketoglutarate or proline, using the Alamar Blue assay. Incubation was
331 started at 2×10^6 cell density and the Alamar Blue assay was performed after 48 h at 27°C. The
332 dashed line indicates the concentrations of succinate, malate, α -ketoglutarate or proline (10 mM)
333 used in panel B, which shows growth curves of the PCF in low-proline, high-proline and low-
334 glucose conditions in the presence or not of 10 mM of each metabolite. Cells were maintained in
335 the exponential growth phase (between 10^6 and 10^7 cells/ml), and cumulative cell numbers
336 reflect normalization for dilution during cultivation. In panel C, the PCF trypanosomes were
337 incubated for 6 h in PBS containing 4 mM succinate (S), malate (M) or α -ketoglutarate (K), in
338 the presence or absence of 4 mM $[\text{U-}^{13}\text{C}]$ -proline (P) or $[\text{U-}^{13}\text{C}]$ -glucose (G), before analysis of
339 the spent medium by ^1H -NMR spectrometry. As a control, the cells were also incubated with 4
340 mM $[\text{U-}^{13}\text{C}]$ -proline (P) or $[\text{U-}^{13}\text{C}]$ -glucose (G) alone. The amounts of end-products excreted
341 from the metabolism of proline (black), glucose (grey), succinate (red), malate (green) and α -
342 ketoglutarate (blue) are expressed as μmol excreted/h/mg of protein.

343
344 **The TCA cycle is used to metabolize malate in procyclic trypanosomes**
345 ^1H -NMR spectrometry analyses showed that, in the presence of proline, malate is converted in
346 almost equal amounts to fumarate and succinate (35.9% and 38.6% of the excreted end-

347 products), in addition to alanine and acetate (14.9% and 10.6% of the excreted end-products)
348 (Fig 5A). According to the current view, malate is converted by the malic enzymes to pyruvate
349 (step 15 in Fig 1C), a precursor for the production of alanine and acetate, as described above
350 (steps 4 and 16-18). As observed for the metabolism of succinate, production of acetate from
351 malate is abolished in the *^{RNAi}PDH-E2.i* cell line (Fig 5A), with an accumulation of malate-
352 derived pyruvate and alanine. Malate can also be converted by FHM to fumarate (step 10), which
353 is further reduced to succinate by the mitochondrial NADH-dependent fumarate reductase
354 (FRDm1, step 9). It is to note that the cytosolic (FHC) and glycosomal (FRDg) isoforms of these
355 two enzymes, respectively, could also be involved in succinate production [24,25], justifying the
356 use of the *^{RNAi}FRDg/m1.i* and *^{RNAi}FHC/m.i* double mutants to study the production of succinate
357 from malate. Succinate production from malate was reduced but not abolished in either of these
358 two double mutants, suggesting that PCF uses an alternative pathway in addition to this reducing
359 branch (Fig 5A). Indeed, malate is also reduced to succinate by TCA cycle enzymes (steps 11-14
360 and 5-6), as inferred by diminished secretion of malate-derived succinate in the Δ *aco* (aconitase,
361 step 13) and Δ *kdh-e2* (α -ketoglutarate dehydrogenase subunit E2, step 5) mutant cell lines (Fig
362 5A). Two other lines of evidence supported the utilization of the oxidative branch of the TCA
363 cycle to produce succinate. First, the Δ *kdh-e2* null mutant excreted α -ketoglutarate from malate
364 metabolism. Second, the expected abolition of fumarate production from malate in the
365 *^{RNAi}FHC/m.i* double mutant (Fig 5A), implies that the malate-derived succinate cannot be
366 produced by the fumarate reductase activity, but by the TCA cycle activity. The relatively high
367 flux of malate consumption is probably the consequence of an efficient maintenance of the
368 mitochondrial redox balance, with NADH molecules produced in the oxidative branches
369 (succinate production through the TCA cycle and acetate production) being reoxidized, at least in
370 part, by the reductive branch (succinate production by fumarate reductases). This resembles the
371 malate dismutation phenomenon well described in anaerobic parasites (for reviews see [26,27]).
372 It is of note that, in the presence of proline, succinate was also converted to succinyl-CoA and
373 probably to succinate through the TCA cycle as inferred by the accumulation of excreted non-
374 enriched α -ketoglutarate in the Δ *kdh-e2* null mutant incubated with succinate and [U-¹³C]-
375 proline (Figs 3B and 1B). These data confirmed that the TCA cycle operates as a complete cycle
376 in these growth conditions.

377
378 **Fig. 5. ¹H-NMR analyses of end-products excreted from the metabolism of malate and α -**
379 **ketoglutarate.** Panel A shows ¹H-NMR spectrometry analyses of the exometabolome produced

380 by the parental (WT), ^{RNAi}PDH-E2.i, ^{RNAi}FRDg/m1.i, ^{RNAi}FHc/m.i, Δ aco and Δ kdh-e2 cell lines
381 incubated with 4 mM [U-¹³C]-proline (¹³C-Pro) and 4 mM malate (Mal). The insets show
382 Western blot analyses with the immune sera indicated in the right margin of the parental (WT),
383 the tetracycline-induced (.i) and non-induced (.ni) ^{RNAi}FRDg/m1 and ^{RNAi}FHc/m cell lines, and
384 the Δ aco cell line. Panel B is equivalent to panel A with the parental (WT), ^{RNAi}SDH.i and Δ kdh-
385 e2 cell lines incubated in the presence of [U-¹³C]-proline alone (¹³C-Pro) or with α -ketoglutarate
386 (¹³C-Pro + α KG). Because of high background, ¹³C-enriched 2-hydroxyglutarate produced from
387 [U-¹³C]-proline cannot be quantified, however, asterisks (*) mean that it is detectable. Since the
388 amounts of 2-hydroxyglutarate produced from non-enriched proline are quantifiable, the values
389 are indicated with grey columns when applicable. The excreted amounts are indicated in the
390 truncated columns (nmol/h/mg of protein). The AAT and MDH (control) enzymatic activities of
391 the parental (WT) and the tetracycline-induced (.i) and non-induced (.ni) ^{RNAi}AAT cell lines are
392 shown in panel C. In panel D, the WT and ^{RNAi}AAT.i cells were incubated for 6 h in PBS
393 containing 4 mM proline (Pro) with or without 4 mM [U-¹³C]-alanine (¹³C-Ala), before analysis
394 of the spent medium by ¹H-NMR spectrometry. The amounts of end-products excreted from the
395 metabolism of proline (black) and alanine (pink) are expressed as μ mol excreted/h/mg of protein.
396 Panel E is equivalent to panel B, except that the ^{RNAi}AAT.i is analyzed. Abbreviations: A,
397 acetate; Al, alanine; F, fumarate; G, glutamate; H, 2-hydroxyglutarate; K, α -ketoglutarate; nd,
398 not detectable; M, Malate; O, malate + pyruvate + acetate + alanine; S, succinate; *, detected but
399 not quantifiable.

400

401 **Metabolism of α -ketoglutarate in the presence of proline**

402 To our surprise, ¹H-NMR spectrometry analyses of α -ketoglutarate metabolism showed that its
403 rate of consumption in the presence of equal amounts (4 mM) of proline (~15 μ mole/h/mg of
404 protein) is ~15-times higher compared to that of glucose (~1 μ mole/h/mg of protein), the latter
405 having previously been considered as the most rapidly degraded carbon source by PCF
406 trypanosomes [6]. As observed for the metabolism of succinate and malate, the rate of α -
407 ketoglutarate catabolism is increased in the presence of proline or glucose (Fig 4C). In the
408 presence of proline, α -ketoglutarate is mainly converted to equivalent amounts of succinate and
409 2-hydroxyglutarate (45.5% and 37.2% of the excreted end-products, respectively), with
410 significant amounts of glutamate (8.7%), acetate (3.6%), pyruvate (3.1%) and malate (1.6%), as
411 well as less than 1% of alanine and lactate (Fig 5B). The production of 2-hydroxyglutarate and
412 glutamate from α -ketoglutarate was validated by comparing the exometabolome of the PCF

413 incubated with [U-¹³C]-proline or [U-¹³C]-proline/α-ketoglutarate with 2-hydroxyglutarate and
414 glutamate standards (S2 Fig). According to the current model, succinate is produced from α-
415 ketoglutarate by the successive action of α-ketoglutarate dehydrogenase (KDH, step 5 in Fig 1D)
416 and succinyl-CoA synthetase (SCoAS, step 6). Succinate then feeds production of malate,
417 pyruvate, alanine and acetate (Fig 1D, O for other), as evidenced by their absence in the
418 exometabolome of the ^{RNAi}SDH.i cell line incubated with [U-¹³C]-proline and α-ketoglutarate
419 (Fig 5B).

420 The *Δkdh-e2* null mutant excretes only 2-hydroxyglutarate from metabolism of α-ketoglutarate,
421 suggesting that a single reduction step, catalyzed by an as yet unknown enzyme, produces 2-
422 hydroxyglutarate from α-ketoglutarate [28,29]. It has recently been proposed that 2-
423 hydroxyglutarate detected in the *T. brucei* BSF metabolome results from the promiscuous action
424 of the NADH-dependent malate dehydrogenase on α-ketoglutarate [30]. 2-hydroxyglutarate is
425 also produced from malate and succinate by the *Δkdh-e2* null mutant (Figs 3B and 5A). In
426 addition, revisiting NMR spectrometry data showed that 2-hydroxyglutarate is also excreted by
427 the parental PCF from proline metabolism in the presence of glucose, but not in its absence (Fig
428 2B). It is noteworthy that ¹³C-enriched 2-hydroxyglutarate molecules produced from [U-¹³C]-
429 proline are barely detectable due to high background and observed but not quantifiable in the
430 ^{RNAi}SDH.i and *Δkdh-e2* cell lines (Figs 3B and 5).

431 Since, α-ketoglutarate is produced from glutamate by the AAT transamination reaction (step 4)
432 [11], the ^{RNAi}AAT.i cell line was studied to determine if AAT catalyzes the reverse reaction. The
433 AAT activity was no longer detectable in the ^{RNAi}AAT.i cell line (Fig 5C), however, the
434 catabolism of proline was only 2.5-fold reduced in the ^{RNAi}AAT.i cell line compared to the
435 parental cell line (Fig 5D). In addition, the ^{RNAi}AAT.i cell line still produced glutamate from α-
436 ketoglutarate (Fig 5E). This suggests that an alternative enzyme is involved in the reversible
437 conversion of glutamate to α-ketoglutarate. Interestingly, alanine conversion to acetate, which
438 theoretically requires the AAT activity working in the direction of glutamate production (see Fig
439 1A), was 20-fold reduced in the ^{RNAi}AAT.i cell line (Fig 5D), suggesting that the alternative
440 enzyme is not using alanine as substrate to convert α-ketoglutarate to glutamate and is probably
441 not another aminotransferase showing substrate promiscuity. Thus, the best candidate is the
442 NADH-dependent glutamate dehydrogenase previously described in trypanosomatids [12,31].

443 It is noteworthy that the possible NADH consumption through reduction of α-ketoglutarate to 2-
444 hydroxyglutarate (5.6 ±0.47 μmol produced/h/mg of protein) and glutamate (1.3 ±0.17 μmol

445 produced/h/mg of protein) may compensate NADH production by the KDH reaction (6.8 ± 0.35
446 μmol of succinate produced/h/mg of protein).

447

448 **α -Ketoglutarate rescued the growth defect of the ^{RNAi}PRODH.i and ^{RNAi}AAT.i mutants**

449 We previously showed that proline dehydrogenase (PRODH), which catalyzes the first step of
450 proline catabolism, is important for the growth of the PCF in glucose-depleted conditions [6].
451 Growth of the ^{RNAi}PRODH.i cell line was considerably reduced but not abolished in glucose-
452 depleted conditions, probably because of the residual PRODH activity (Fig 6A) and residual
453 conversion of proline to excreted end-products (Fig 6B). As expected, proline did not rescue
454 growth of the ^{RNAi}PRODH.i mutant in glucose-depleted conditions. However, succinate and
455 malate improved growth of the mutant and more importantly α -ketoglutarate completely rescued
456 its growth (Fig 6C), even in the presence of 12 mM proline (Fig 6D). Unfortunately, we failed to
457 obtain the Δprodh null mutant in standard glucose-rich conditions, with or without 10 mM α -
458 ketoglutarate, probably because minimal proline catabolism is required even in the presence of
459 glucose. As mentioned above, proline metabolism was 2.5-fold reduced in the ^{RNAi}AAT.i mutant
460 cell line (Fig 5D). This caused a slight growth defect in glucose-depleted conditions that was
461 rescued by the addition of α -ketoglutarate, as observed for the ^{RNAi}PRODH.i mutant (Fig 7B).
462 Collectively, these data suggest that metabolism of α -ketoglutarate, and to a lesser extent in the
463 case of the ^{RNAi}PRODH.i cell line, succinate and malate, compensate for the lack of proline
464 metabolism. To confirm these data, the ability of these carbon sources to replace proline was
465 tested under long-term growth conditions. Because of the auxotrophy of *T. brucei* for proline,
466 which is necessary for protein biosynthesis, the growth medium contained 0.2 mM proline. In
467 these conditions, the growth defect observed in the absence of an additional carbon source is
468 partially rescued with the same efficiency by 10 mM α -ketoglutarate, glucose, succinate and
469 malate (S3 Fig). Interestingly, the growth rate in low-proline conditions is the same whether in
470 the presence of glucose or malate/succinate/ α -ketoglutarate, thus confirming that these TCA
471 cycle intermediates are excellent carbon and energy sources for PCF.

472

473 **Fig. 6. Growth of the ^{RNAi}PRODH.i mutant is rescued by α -ketoglutarate.** The efficiency of
474 RNAi-mediated downregulation of PRODH expression in the tetracycline-induced (.i) or non
475 induced (.ni) ^{RNAi}PRODH cell line, as well as in the parental cell line (WT) was determined by
476 the PRODH activity assay (panel A) and ¹H-NMR quantification of end-products excreted from
477 metabolism of proline and glucose in two independent experiments (panel B). Panel C shows

478 growth curves of the ^{RNAi}PRODH.i cell line in glucose-depleted medium containing 2 mM
479 proline, in the presence (colored circles) or absence (open circles) of 10 mM α -ketoglutarate,
480 malate, succinate or proline. Cells were maintained in the exponential growth phase and
481 cumulative cell numbers reflect normalization for dilution during cultivation. The effect of 10
482 mM succinate, malate, α -ketoglutarate or proline on growth of the parental and ^{RNAi}PRODH.i cell
483 lines in glucose-depleted medium containing 2 mM proline, using the Alamar Blue assay
484 described in Figure 4, is shown in panel D.

485

486 **α -Ketoglutarate is toxic if not metabolized at a high rate**

487 As mentioned above, proline metabolism was strongly affected in the $\Delta kdh-e2$ mutant, with only
488 production of α -ketoglutarate and 2-hydroxyglutarate (Fig 5A-B). As a consequence, growth of
489 the $\Delta kdh-e2$ mutant was compromised in glucose-depleted medium containing 2 mM or 10 mM
490 proline, while the addition of 10 mM malate or succinate rescued this growth phenotype (Fig 7A-
491 B). However, addition of α -ketoglutarate at concentrations as low as 1 mM was detrimental for
492 the survival of the $\Delta kdh-e2$ mutant (Fig 7A-B). This toxic effect of α -ketoglutarate was
493 confirmed by the analysis of the ^{RNAi}SDH.i and ^{RNAi}SCoAS.i mutants, which are also affected in
494 α -ketoglutarate metabolism. Indeed, growth of these two mutant cell lines was reduced in the
495 presence of α -ketoglutarate (Fig 7B). It is also of note that expression of SCoAS was not fully
496 abolished in the ^{RNAi}SCoAS.i, which may explain the moderate reduction in its growth (Fig 7C).
497 These data suggest that accumulation of α -ketoglutarate, or one of its metabolic derivatives, is
498 toxic to PCF trypanosomes. Indeed, we cannot exclude that reduction of α -ketoglutarate to
499 isocitrate, citrate or one of their metabolic products is responsible for this phenotype (see Fig
500 1D). To block the possible citrate/isocitrate production from α -ketoglutarate in the $\Delta kdh-e2$ and
501 ^{RNAi}SCoAS backgrounds, the *IDHm* gene was knocked-down or knocked-out to produce the
502 $\Delta kdh-e2$ /^{RNAi}IDHm and $\Delta idhm$ /^{RNAi}SCoAS cell lines, respectively. Growth of these tetracycline-
503 induced double mutants was strongly impaired by the addition of α -ketoglutarate as observed for
504 the $\Delta kdh-e2$ and ^{RNAi}SCoAS.i single mutants, while α -ketoglutarate stimulated growth of the
505 $\Delta idhm$ as observed for the parental cell line (Fig 7A). This confirmed that it is accumulation of
506 α -ketoglutarate itself that is responsible for this phenomenon.

507 It is noteworthy that accumulation of succinate was not toxic for trypanosomes, as exemplified
508 by the absence of effect of 10 mM succinate on growth of the ^{RNAi}SDH.i cell line (Fig 7B), which
509 was no longer able to metabolize succinate (Fig 3B). As expected, malate stimulated growth of
510 this mutant (Fig 7B).

511
512 **Fig. 7. α -ketoglutarate is toxic for the $\Delta kdh-e2$, RNAi SCoAS.i and RNAi SDH.i cell lines.** Panel
513 A compares the effect of succinate, malate, α -ketoglutarate or proline (10 mM) on growth of the
514 parental and mutant cell lines in glucose-depleted medium containing 2 mM proline, using the
515 Alamar Blue assay described in Figure 4. Panel B shows growth curves of the RNAi AAT, $\Delta kdh-e2$,
516 RNAi SDH and RNAi SCoAS cell lines incubated in glucose-depleted medium containing 2 mM
517 proline, in the presence (colored circles) or absence (open circles) of α -ketoglutarate, malate,
518 succinate or proline (10 mM) (.i, tetracycline-induced cells; .ni, non induced cells). Cells were
519 maintained in the exponential growth phase and cumulative cell numbers reflect normalization
520 for dilution during cultivation. Panel C shows Western blot analyses with the immune sera
521 indicated in the right margin of the parental (WT), $\Delta idhm$ and tetracycline-induced (.i) and non-
522 induced (.ni) RNAi SCoAS, $\Delta idhm$ / RNAi SCoAS and $\Delta kdh-e2$ / RNAi IDHm cell lines.

523
524 **α -Ketoglutarate stimulates growth of epimastigote-like forms**
525 To investigate whether TCA cycle intermediates are also carbon sources for the epimastigote
526 trypanosomes, we took advantage of the *in vitro*-induced differentiation approach developed by
527 Kolev *et al.*, in which the differentiation of PCF to epimastigotes and then into metacyclics is
528 triggered by overexpression of a single RNA binding protein (RBP6) [32]. In order to increase
529 the proportion of epimastigotes, we selected a cell line expressing relatively low levels of RBP6,
530 since the *in vitro*-induced differentiation of epimastigotes into metacyclics depends on strong
531 overexpression of RBP6 [32]. Upon induction of RBP6 expression, the selected OE RBP6.i cell
532 line expressed the BARP (*brucei* alanine rich proteins) epimastigote differentiation marker [33],
533 as well as the alternative oxidase (TAO), which has recently been described as strongly
534 overexpressed in epimastigotes [34] (Fig 8A). This was confirmed by microscopy three days post
535 induction, since 54% of the cells showed an epimastigote-like repositioning of the kinetoplast to
536 reside close to the nucleus, while the other cells are procyclic-like (S4 Fig). In contrast no
537 metacyclics were observed after eight days of induction, which is consistent by the stable
538 expression of calflagin (Fig. 8A), a 10-fold upregulated flagellar protein in the bloodstream
539 forms compared to procyclics [35]. We thus concluded that this tetracycline-induced OE RBP6
540 cell line is enriched in epimastigote-like forms and/or forms in the process of becoming
541 epimastigotes, whose carbon source requirements can be investigated. Growth of the OE RBP6.i
542 cells stopped after 6 days in the presence of 2 mM proline, while growth of non-induced
543 OE RBP6.ni cells was not affected. Interestingly, this growth defect is rescued by the addition of

544 10 mM proline or 10 mM α -ketoglutarate, but not the same quantity of succinate or malate. We
545 confirmed that the expression profile of BARP and TAO is not affected by the presence of 10
546 mM α -ketoglutarate or 10 mM proline (Fig 8C) and ~50% of the cells showed an epimastigote-
547 like repositioning of the kinetoplast 3 days post-induction. This data suggested that the amount
548 of proline present in the midgut of the fly (1-2 mM) might be not sufficient to sustain growth of
549 the epimastigotes and/or procyclic cells differentiating into epimastigotes and that additional
550 carbon sources, such as α -ketoglutarate, should be needed to complete the development of the
551 parasite *in vivo*.

552
553 **Fig. 8. Large amounts of carbon sources are required for the growth of epimastigote-like**
554 **cells.** Panels A and C show Western blot analyses with the indicated immune sera (BARP, *brucei*
555 alanine rich proteins; TAO, terminal alternative oxidase) of the ^{OE}RBP6 cell line upon
556 tetracycline induction and growth in low-proline conditions (2 mM) after addition (panel B) or
557 not (panel C) of 10 mM α -ketoglutarate or 10 mM proline. HSP60 was used as loading control.
558 Panel B shows growth curves of the tetracycline-induced (.i) and non-induced (.ni) ^{OE}RBP6 cell
559 line, in the presence of 2 mM proline, with or without addition of 10 mM α -ketoglutarate,
560 succinate, malate, or proline. The curves are representative replicates of three different
561 experiments.

562

563

564 Discussion

565 Procyclic trypanosomes are thought to have developed a central metabolic network adapted to
566 the metabolism of three main carbon sources for their energy, *i.e.* glucose, glycerol and proline
567 [5,10,36]. Here we show that the parasite efficiently metabolizes a number of other carbon
568 sources, including pyruvate, alanine and the TCA cycle intermediates succinate, malate and α -
569 ketoglutarate. Several reports previously described the ability of African trypanosomes to
570 consume and metabolize TCA cycle intermediates. For instance, α -ketoglutarate has been
571 described to stimulate respiration and to sustain mobility of the stumpy forms of *T. brucei*, which
572 are a growth-arrested transition form found in the bloodstream that are pre-adapted to
573 differentiation into PCF [37–40]. In the 1960s, Riley showed that TCA cycle intermediates,
574 including α -ketoglutarate, succinate, malate and fumarate, stimulate oxygen consumption of *T.*
575 *brucei rhodesiense* culture forms (PCF) [36]. However, the metabolism of these TCA cycle
576 intermediates by PCF trypanosomes has not been investigated so far in the context of the insect-

577 like environment, that is to say in the absence of glucose but with proline present in the low
578 millimolar range (1-2 mM), as described for the midgut of the tsetse fly [20]. Here we showed
579 that in the presence of 2 mM proline, consumption and metabolism of succinate, malate and α -
580 ketoglutarate takes place. More importantly, addition of 1-10 mM of any one of these three TCA
581 cycle intermediates stimulates growth of the parasite and rescues growth of the parasite in the
582 presence of 2 mM and 0.2 mM proline, respectively.

583 We took advantage of the unexpectedly high mitochondrial metabolic capacity developed by the
584 PCF trypanosomes in the presence of α -ketoglutarate, succinate or malate to carry out a detailed
585 analysis of the TCA cycle and its branched pathways. This allowed us to show (i) the high
586 metabolic capacity of the malate/ α -ketoglutarate branch of the TCA cycle, (ii) the toxicity of α -
587 ketoglutarate intracellular accumulation and (iii) the production of 2-hydroxyglutarate from
588 metabolism of α -ketoglutarate and proline. (i) Van Weelden *et al.* previously demonstrated that
589 PCF trypanosomes cultured in rich medium do not need to oxidize glucose *via* a complete TCA
590 cycle fed with glucose-derived acetyl-CoA [15]. Indeed, they showed that the growth rate of the
591 Δ *aco* and parental cell lines was identical in the standard glucose-rich medium and, more
592 importantly, the malate/ α -ketoglutarate branch of the TCA cycle (steps 11-14 in Fig 1A) showed
593 no significant activity in PCF trypanosomes, as measured by [14 C]-CO₂ release from labeled
594 glucose. However, these data did not exclude a functional malate/ α -ketoglutarate branch, which
595 is used under specific nutritional conditions, or in particular developmental stages, and the
596 sensitivity of the assay used in that work was limited. Here we have demonstrated the
597 functionality of this metabolic branch by forcing the parasite to use it in the presence of 10 mM
598 malate and 2 mM proline. In these conditions, malate is converted to succinate *via* both the
599 reducing (steps 9-10 in Fig 1C) and oxidative (steps 11-14 and 5-6) branches of the TCA cycle.
600 Indeed, fumarate production from malate is abolished in the ^{*RNAi*}FHc/m.i mutant (step 10), while
601 succinate production from malate is little affected, and succinate production is only reduced by
602 1.8-fold in the ^{*RNAi*}FRDg/m.i mutant (step 9). These data can only be explained by a significant
603 metabolic flux through the malate/ α -ketoglutarate branch of the TCA cycle fed with extracellular
604 malate. Since this branch of the TCA cycle does not seem to be important for their energy in
605 standard culture conditions in the wild type PCF trypanosomes [15], its main function in the
606 procyclic trypanosomes could be the production of citrate and/or isocitrate to supply other
607 metabolic pathways. This hypothesis is consistent with the glycosomal localization of the IDHg
608 isoform, which requires isocitrate for NADH and/or NADPH production within the organelle
609 [41]. However, as opposed to most eukaryotes, trypanosomes do not use TCA-cycle derived

610 citrate to produce the precursor of *de novo* fatty acid biosynthesis, *i.e.* acetyl-CoA, in the cytosol.
611 The parasites lack the key enzyme of this pathway, *i.e.* cytosolic acetyl-CoA lyase, and instead
612 use the cytosolic AMP-dependent acetyl-CoA synthetase to produce acetyl-CoA from acetate
613 [42]. Interestingly, Dolezelova *et al.* recently took advantage of an *in vitro* differentiation assay
614 based on RBP6 overexpression to show that all of the enzymes of the malate/ α -ketoglutarate
615 branch of the TCA cycle are strongly overexpressed upon differentiation into the epimastigote
616 forms of *T. brucei* [34]. This suggests that this branch of the TCA cycle and/or the full TCA
617 cycle is required for epimastigotes and/or during differentiation of procyclics into epimastigotes.
618 (ii) Accumulation of the TCA cycle intermediate, α -ketoglutarate is toxic for PCF, while
619 accumulation of succinate in the ^{RNAi}SDH.i mutant cultivated in the presence of 10 mM succinate
620 is not toxic. α -Ketoglutarate toxicity was deduced from the death of the $\Delta kdh-e2$ and $\Delta kdh-$
621 $e2$ /^{RNAi}IDHm.i mutants in the presence of α -ketoglutarate, which is not efficiently metabolized in
622 these mutants compared to the parental cell line. α -Ketoglutarate is a key metabolite at the
623 interface between metabolism of carbon and nitrogen [43], which has recently emerged as a
624 master regulator metabolite in prokaryotes and cancer cells [44,45]. Consequently, intracellular
625 accumulation of large amounts of α -ketoglutarate could affect several essential pathways, by
626 mechanisms that are currently unknown. (iii) 2-Hydroxyglutarate is a five-carbon dicarboxylic
627 acid occurring naturally in animals, plants, yeasts and bacteria. It has recently been described as
628 an epigenetic modifier that governs T cell differentiation and plays a role in cancer initiation and
629 progression [28,46]. This metabolite was also detected in the metabolome of BSF trypanosomes,
630 being derived from the metabolism of glutamate [30]. Here we showed that 2-hydroxyglutarate
631 represents 37% of the total end-products excreted by PCF from catabolism of α -ketoglutarate,
632 with an excretion rate of 2-hydroxyglutarate 3.4 times higher than that of end-products from
633 glucose metabolism (6.77 *versus* 2.02 μ mole/h/mg of protein). This highlights the high capacity
634 of the enzyme responsible for α -ketoglutarate reduction to 2-hydroxyglutarate. This reaction
635 probably results from the promiscuous action of malate dehydrogenase on α -ketoglutarate or
636 from oncogenic mutations in isocitrate dehydrogenase enzymes, as previously described in
637 mammalian cells [29,47]. This NADH-consuming reaction compensates for the NADH-
638 producing reactions involved in the production of other end-products excreted from α -
639 ketoglutarate metabolism, and may therefore explain the very high α -ketoglutarate metabolic
640 flux. Indeed, maintenance of the mitochondrial redox balance required for α -ketoglutarate
641 metabolism is performed by fast-acting substrate level reactions, with little or no involvement of
642 the respiratory chain, which operates at a lower rate compared to substrate level reactions. Most

643 cells express 2-hydroxyglutarate dehydrogenase enzymes (2HGDH), which irreversibly catalyse
644 the reverse oxidative reaction in order to prevent the loss of carbon moieties from the TCA cycle
645 and would protect from the accumulation of 2-hydroxyglutarate [28]. The *T. brucei* genome
646 contains a putatively annotated *2HGDH* gene (Tb927.10.9360), however since 2-
647 hydroxyglutarate is produced in high quantities in PCF organisms its role in these cells is
648 uncertain.

649 Trypanosomatids convert carbon sources to partially oxidized end-products that are excreted into
650 the environment [5]. Some of these metabolites constitute good alternative carbon sources for the
651 parasite, as exemplified by efficient metabolism of alanine by *T. cruzi*, while this amino acid is
652 also excreted from glucose breakdown [48]. Here, we report that end-products excreted from the
653 metabolism of glucose by PCF trypanosomes, such as succinate, alanine and pyruvate, are re-
654 consumed after glucose has been used up. Indeed, ¹³C-enriched succinate and alanine excreted
655 from catabolism of [U-¹³C]-glucose are re-consumed and converted to ¹³C-enriched acetate after
656 glucose depletion. This phenomenon resembles the “acetate switch” which has been well
657 described in prokaryotes, in which abundant or preferred nutrients, such as glucose, are first
658 fermented to acetate, followed by the import and utilization of that excreted acetate to enhance
659 survival of the cells [49]. This “acetate switch” occurs when cells deplete their environment of
660 acetate-producing carbon sources.

661 We previously described that PCF trypanosomes cultivated in rich conditions use ~5 times more
662 glucose than proline to feed their central carbon metabolism, and switch to proline metabolism in
663 the absence of glucose by increasing its rate of consumption up to 5 fold [6,7]. Indeed, glucose is
664 first fermented to excreted acetate, succinate, alanine and pyruvate, before switching to proline
665 that is primarily metabolized in the mitochondrion with an increased contribution of the
666 respiratory chain. Here we showed that this “proline switch” is accompanied by the re-utilization
667 and conversion of glucose-derived end-products (succinate, pyruvate and alanine) to acetate. As
668 opposed to bacteria or yeasts, however, acetate does not feed carbon metabolism of PCF and is
669 the ultimate excreted end-product from the breakdown of the different carbon sources, including
670 succinate and alanine. The ratio between the two main excreted end-products from glucose
671 metabolism (acetate/succinate) has been reported to be between 0.3 and 4 in different studies
672 [15,25], which has been interpreted to reflect a high flexibility of flux distribution between the
673 acetate and succinate branches of the metabolic network [22,50]. In light of our observations,
674 however, it appears that the conversion of excreted glucose-derived succinate to excreted acetate,
675 following uptake and further metabolism of succinate, provides an alternative explanation for
676 these heterogeneous data.

677 The *in vitro* differentiation model driven by overexpression of RBP6 was instrumental in
678 showing that epimastigotes and/or cells in the process of differentiating into epimastigotes have a
679 higher demand for carbon sources than procyclic trypanosomes to feed their central carbon
680 metabolism. Indeed, a recent analysis of the proteome and metabolic capability showed that
681 enzymes involved in proline catabolism, as well as mitochondrial respiratory capacity, are
682 upregulated in the epimastigote-enriched population when compared to procyclic trypanosomes.
683 This suggests an increased consumption of carbon sources, probably to meet an increased energy
684 demand [34]. Consistent with these observations, our data demonstrated that growth of
685 epimastigote-like cells, in contrast to that of procyclic cells, is affected by the presence of
686 relatively small amounts of proline (2 mM), which corresponds to the level detected in the insect
687 vector. Interestingly, adding 10 mM proline or 10 mM α -ketoglutarate restored growth,
688 suggesting that this higher demand for carbon and energy sources may be supported by carbon
689 sources other than proline, such as α -ketoglutarate. This increased demand for carbon/energy
690 may contribute to the production of reactive oxygen species involved in the differentiation
691 process of the parasite [34]. Alternatively, inhospitable organs of the fly or structures difficult to
692 cross, such as the proventriculus, may require increased catabolic capacity. Indeed, the
693 proventriculus is an active immune tissue of the insect that represents a hurdle to the spread of
694 trypanosomes from the midgut to the salivary glands, since only a few trypanosomes can pass
695 through it. Unfortunately, with the exception of amino acids [20], the content of metabolites in
696 the tsetse midgut, including the proventriculus, has not been studied so far. TCA cycle
697 intermediates could be present in significant amounts where, for example, tsetse resident
698 symbionts such as *Sodalis glossinidius* metabolize N-acetylglucosamine and glutamine to
699 produce partially oxidized end-products, which are released to the midgut lumen of the fly [18].
700 These may then promote trypanosome development. An exhaustive analysis of the metabolite
701 content of the intestine of naive and infected insects is necessary to deepen our understanding of
702 the role played by TCA cycle intermediates and other carbon sources in the development of
703 trypanosomes in tsetse flies.

704

705

706 **Materials and Methods**

707 **Trypanosomes and cell cultures**

708 The procyclic form of *T. brucei* EATRO1125.T7T (TetR-HYG T7RNAPOL-NEO) and AnTat
709 1.1 were cultured at 27°C in SDM79 medium containing 10% (v/v) heat inactivated fetal calf

710 serum and 5 µg/ml hemin [51] and in the presence of hygromycin (25 µg/ml) and neomycin (10
711 µg/ml). All mutant cell lines have initially been produced and cultivated in the standard SDM79
712 medium. Alternatively, the cells were cultivated in a glucose-depleted medium derived from
713 SDM79 supplemented with 50 mM N-acetylglucosamine, a specific inhibitor of glucose
714 transport that prevents consumption of residual glucose [13]. Control growth conditions in the
715 presence of glucose were performed in glucose-depleted conditions, in which the glucose
716 transport inhibitor N-acetylglucosamine was omitted and 10 mM glucose was added. The growth
717 was followed by counting the cells daily with a Guava EasyCyte™ cytometer. The Alamar Blue
718 assay was used to study the effect of metabolites on parasite growth. To do this, cells at a final
719 density of 2×10^6 cells/ml were diluted in 200 µl of glucose-depleted medium supplemented
720 with 6 mM proline/10 mM glucose, 2 mM proline or 12 mM proline containing 1 µM to 100 mM
721 of the analyzed metabolite and incubated for 48 h at 27°C in microplates, before adding 20 µl of
722 0.49 mM Alamar Blue (Resazurin). Measurement of fluorescence was performed with the
723 microplate reader Fluostar Optima (BMG Labtech) at 550 nm excitation wavelength and 600 nm
724 emission wavelength as previously described [23].

725

726 **Inhibition of gene expression by RNAi**

727 The inhibition by RNAi of gene expression in the PCF trypanosomes was performed by
728 expression of stem-loop “sense/antisense” (SAS) RNA molecules of the targeted sequences
729 introduced into the pLew100 or a single fragment in the p2T7^{Ti}-177 expression vectors (kindly
730 provided by E. Wirtz and G. Cross and by B. Wickstead and K. Gull, respectively) [52,53].
731 Plasmids pLew-FRDg/m1-SAS, p2T7-FHc/m-SAS, pLew-SDH-SAS, pLew-PDH-E2-SAS,
732 pLew-AAT-SAS, p2T7-PRODH were used to generate the ^{RNAi}FRDg/m1-B5 [24], ^{RNAi}FHc/m-
733 F10 [25], ^{RNAi}SDH [7], ^{RNAi}PDH-E2 [7], ^{RNAi}AAT [11] and ^{RNAi}PRODH [6] cell lines, as
734 previously reported [54]. The ^{RNAi}AAT and ^{RNAi}PRODH mutants produced in the 29-13 cell line
735 (derived from strain 427) and the other RNAi cell lines obtained in the EATRO1125.T7T
736 background were grown in SDM79 medium containing hygromycin (25 µg/ml), neomycin (10
737 µg/ml) and phleomycin (5 µg/ml). A 591 bp fragment of the beta subunit of SCoAS
738 (Tb927.10.7410) was PCR amplified and cloned into the p2T7^{Ti}-177 plasmid using the BamHI
739 and HindIII restriction sites (p2T7^{Ti}-177-SCoAS). Procyclic EATRO1125.T7T cells were
740 transfected with the p2t7-177-SCoAS plasmid to generate the ^{RNAi}SCoAS cell line. To assemble
741 p2T7^{Ti}-177_IDHm^{RNAi}(ble), a 1127 bp fragment of IDHm (Tb927.8.3690) was amplified
742 (primers IDHm_fwd: TGTCTACAACACGTCCAA and IDHm_rev BamHI:
743 CGATAggatccGATGGTTTTGATCGTTGC) from genomic AnTat1.1 DNA and cloned into the

744 p2T7^{Ti}-177 plasmid using the BamHI and HindIII restriction sites.

745

746 **Production of null mutants**

747 The *ASCT* gene was replaced by the blasticidin/puromycin resistance markers to generate the
748 previously reported $\Delta asct$ null mutant [14]. The Δach /^{RNAi}ASCT cell line was generated by
749 introducing the pLew-ASCT-SAS plasmid in the *ach* background [14]. To delete the genes
750 encoding the subunit E2 of KDH (KDH-E2), the resistance markers blasticidin (BLA) and
751 puromycin (PAC) were PCR amplified using long primers with 80 bp corresponding to the
752 5'UTR and 3'UTR region of the *KDH-E2* gene (Tb927.11.9980). To replace the two *KDH-E2*
753 alleles, the EATRO1125.T7T PCF was transfected with 10 μ g of purified PCR products
754 encoding the resistance markers flanked by UTR regions. The selected $\Delta kdh-e2::PAC/\Delta kdh-$
755 $e2::BLA$ cell line was named $\Delta kdh-e2$. The cell line $\Delta kdh-e2$ /^{RNAi}IDHm was generated by
756 transfection of p2T7^{Ti}-177_IDHm^{RNAi}(ble) into $\Delta kdh-e2$ and selection with phleomycin. For
757 generation of a homozygous Δaco cell line in the EATRO1125.T7T background, previously
758 reported targeting constructs [15] were modified by replacing the neomycin and hygromycin
759 selection markers with blasticidin and puromycin, respectively. For homozygous deletion of
760 *IDHm* (Tb927.8.3690), the EATRO1125.T7T line was transfected with targeting constructs
761 having the blasticidin and puromycin selection marker cassettes flanked by *IDHm* 5'-UTR (797
762 bp) and 3'-UTR (876 bp) sequences, amplified from genomic DNA of strain MiTat1.4. The
763 selected $\Delta idhm::PAC/\Delta idhm::BLA$ cell line was named $\Delta idhm$. The $\Delta idhm$ null mutant was
764 transfected with the p2T7^{Ti}-177-SCoAS plasmid to generate the $\Delta idhm$ /^{RNAi}SCoAS cell line.

765

766 **In vitro differentiation of PCF expressing RBP6**

767 The *RBP6* gene was amplified by PCR and cloned via HindIII/BamHI into the pLew100v5b1d
768 vector (pLew100v5 modified with a blasticidin resistance gene *BSD*) [23]. The
769 EATRO1125.T7T cell line was transfected with the pLew100v5-RBP6 linearized with NotI in
770 pools to generate the ^{OE}RBP6. *In vitro* differentiation experiments were done as described in
771 [23,32] in SDM79 medium without glucose in the presence of 50 mM *N*-acetyl-D-glucosamine
772 and 10% (v/v) heat-inactivated fetal calf serum.

773

774 **Analysis of excreted end-products from the metabolism of carbon sources by proton NMR**

775 2×10^7 *T. brucei* PCF cells were collected by centrifugation at 1,400 g for 10 min, washed once
776 with phosphate-buffered saline (PBS) and incubated in 1 ml (single point analysis) of PBS
777 supplemented with 2 g/l NaHCO₃ (pH 7.4). For kinetic analysis, 1×10^9 cells were incubated in

778 15 ml under the same conditions. Cells were maintained for 6 h at 27°C in incubation buffer
779 containing one or two ¹³C-enriched or non-enriched carbon sources. The integrity of the cells
780 during the incubation was checked by microscopic observation. The supernatant (1 ml) was
781 collected and 50 µl of maleate solution in D₂O (10 mM) was added as internal reference. H-
782 NMR spectra were performed at 500.19 MHz on a Bruker Avance III 500 HD spectrometer
783 equipped with a 5 mm cryoprobe Prodigy. Measurements were recorded at 25°. Acquisition
784 conditions were as follows: 90° flip angle, 5,000 Hz spectral width, 32 K memory size, and
785 9.3 sec total recycle time. Measurements were performed with 64 scans for a total time close to
786 10 min 30 sec. Resonances of the obtained spectra were integrated and metabolites
787 concentrations were calculated using the ERETIC2 NMR quantification Bruker program. The
788 identification of 2-hydroxyglutarate in some samples was duly confirmed from H-NMR analyses
789 carried out at 800 MHz, after spiking with the pure compound.

790

791 **Western blot analyses**

792 Total protein extracts (5 x 10⁶ cells) were separated by SDS-PAGE (10%) and immunoblotted on
793 TransBlot Turbo Midi-size PVDF Membranes (Bio-Rad) [55]. Immunodetection was performed
794 as described [55,56] using as primary antibodies, the rabbit anti-ASCT (1:500) [57], anti-
795 aldolase (1:10,000) [58], anti-PPDK (1:500) [54], anti-ENO (1:100,000, gift from P. Michels,
796 Edinburgh, UK), anti-FRD (1:100) [24], anti HSP60 (1:10,000) [59], anti-RBP6 (1:500, gift from
797 C. Tschudi, New Haven, USA), anti BARP (1:2,500, gift from I. Roditi, Bern, Switzerland) [33],
798 anti-calflagin (1:1,500) or the mouse anti-PDH-E2 (1:500) [21], anti-TAO 7D3 (1:100, gift from
799 M. Chaudhuri, Nashville, USA) [60] and anti-FH (1:100) [25]. Rabbit anti-IDHm was raised
800 against recombinant His-tagged full length *T. brucei* IDHm expressed in and purified from *E.*
801 *coli*. After intradermal immunization with Freund's complete adjuvant, 12 boosts were required
802 until final bleeding after 180 days (custom immunization by Pineda, Berlin). The recombinant
803 full length SCoAS subunit β with N-terminal 6x His tag was affinity-purified from *E. coli* under
804 native conditions and sent to Davids Biotechnology (Regensburg, Germany) for polyclonal
805 antibody production. Anti-rabbit or anti-mouse IgG conjugated to horseradish peroxidase (Bio-
806 Rad, 1:5,000 dilution) were used as secondary antibody and detected using the Clarity Western
807 ECL Substrate as described by the manufacturer (Bio-Rad). Images were acquired and analyzed
808 with the ImageQuant LAS 4000 luminescent image analyzer.

809

810 **Enzymatic activity assays**

811 For PRODH and SDH activities, Log phase PCF cells were harvested and washed twice with

812 STE buffer (25 mM Tris-HCl, pH 7.4, 1 mM EDTA, 0.25 M sucrose, Protease inhibitors) and
813 treated with 0.35 mg digitonin per mg of protein during 4 min at room temperature. After
814 centrifugation 2 min at 12,000 x g, the enzymatic activities were determined in the pellets
815 resuspended in STE. Proline dehydrogenase (PRODH) and succinate dehydrogenase activities
816 (SDH) were measured following the reduction of the electron-accepting dye
817 dichlorophenolindophenol (DCPIP) at 600 nm [61]. The assays contained 11 mM MOPS pH 7.5,
818 11 mM MgCl₂, 11% glycerol, 56 μM DCPIP, 0.9 mM PMS, 10 mM of proline for PRODH
819 activity or 20 mM of succinate for SDH activity. The alanine aminotransferase (AAT) activity
820 was measured following the oxidation of NADH at 340 nm [62]. The malate dehydrogenase
821 (MDH) activity was determined as a control [63].

822

823

824 **Acknowledgements**

825 We thank Paul A. Michels (Edinburgh, Scotland), Christian Tschudi (New Haven, USA), Minu
826 Chaudhuri (Nashville, USA) and Isabel Roditi (Bern, Switzerland) for providing us with the anti-
827 enolase, anti-RBP6, anti-TAO and anti-BARP immune sera, respectively. F. Bringaud's group
828 was supported by the Centre National de la Recherche Scientifique (CNRS), the Université de
829 Bordeaux, the ANR through the grants GLYCONOV (grant number ANR-15-CE15-0025-01)
830 and ADIPOTRYP (grant number ANR-19) and the Laboratoire d'Excellence (LabEx) ParaFrap
831 ANR-11-LABX-0024. M. Barrett's group was supported by the Wellcome Trust core grant to the
832 Wellcome Centre of Integrative Parasitology (grant number 104111/Z/14/Z). A. M. Silber's
833 group is supported by FAPESP (grant number 2016/06034-2) and CNPq (grants number
834 308351/2013-4 and 404769/2018-7). A. M. Silber and M. Barrett are funded by a joint FAPESP-
835 MRC/UKRI-NEWTON FUND award: "Bridging epigenetics, metabolism and cell cycle in
836 pathogenic trypanosomatids" (grant number 2018/14432-3), A. Zikova's group by Grant Agency
837 of the Czech Republic (20-14409S) and ERD fund (CZ.02.1.01/0.0/0.0/16_019/0000759) and M.
838 Boshart's group was funded by DFG SPP1131, and BayFrance agency supported collaboration
839 between the Bordeaux and Munich labs. MetaboHub-MetaToul (Metabolomics & Fluxomics
840 facilities, Toulouse, France, <http://www.metatoul.fr>) is supported by the ANR grant
841 MetaboHUB-ANR-11-INBS-0010. JCP is grateful to INSERM for funding a temporary full-time
842 researcher position.

843

844

845 References

- 846 1. Buscher P, Cecchi G, Jamonneau V, Priotto G. Human African trypanosomiasis. *Lancet*.
847 2017;390: 2397–2409. doi:10.1016/S0140-6736(17)31510-6
- 848 2. Opperdoes FR, Borst P. Localization of nine glycolytic enzymes in a microbody-like
849 organelle in *Trypanosoma brucei*: the glycosome. *FEBS Lett*. 1977;80: 360–4. doi:0014-
850 5793(77)80476-6 [pii]
- 851 3. Visser N, Opperdoes FR. Glycolysis in *Trypanosoma brucei*. *Eur J Biochem*. 1980;103:
852 623–32.
- 853 4. Mazet M, Morand P, Biran M, Bouyssou G, Courtois P, Daulouede S, et al. Revisiting the
854 central metabolism of the bloodstream forms of *Trypanosoma brucei*: production of acetate
855 in the mitochondrion is essential for parasite viability. *PLoS Negl Trop Dis*. 2013;7: e2587.
856 doi:10.1371/journal.pntd.0002587 PNTD-D-13-01131 [pii]
- 857 5. Bringaud F, Riviere L, Coustou V. Energy metabolism of trypanosomatids: adaptation to
858 available carbon sources. *Mol Biochem Parasitol*. 2006;149: 1–9. doi:S0166-
859 6851(06)00115-0 [pii] 10.1016/j.molbiopara.2006.03.017
- 860 6. Lamour N, Riviere L, Coustou V, Coombs GH, Barrett MP, Bringaud F. Proline metabolism
861 in procyclic *Trypanosoma brucei* is down-regulated in the presence of glucose. *J Biol Chem*.
862 2005;280: 11902–11910.
- 863 7. Coustou V, Biran M, Breton M, Guegan F, Riviere L, Plazolles N, et al. Glucose-induced
864 remodeling of intermediary and energy metabolism in procyclic *Trypanosoma brucei*. *J Biol*
865 *Chem*. 2008;283: 16342–54. doi:M709592200 [pii] 10.1074/jbc.M709592200
- 866 8. Mantilla BS, Marchese L, Casas-Sanchez A, Dyer NA, Ejeh N, Biran M, et al. Proline
867 metabolism is essential for *Trypanosoma brucei brucei* survival in the tsetse vector. *PLoS*
868 *Pathog*. 2017;13: e1006158. doi:10.1371/journal.ppat.1006158
- 869 9. Bursell E. The role of proline in energy metabolism. New York: Plenum Press; 1981.
- 870 10. Obungu VH, Kiara JK, Olembo NK, Njobu MR. Pathways of glucose catabolism on
871 procyclic *Trypanosoma congolense*. *Indian J Biochem Biophys*. 1999;36: 305–11.
- 872 11. Spitznagel D, Ebikeme C, Biran M, Nic A, Bhaird N, Bringaud F, Henehan GT, et al.
873 Alanine aminotransferase of *Trypanosoma brucei* - a key role in proline metabolism in
874 procyclic life forms. *FEBS J*. 2009;276: 7187–7199. doi:EJB7432 [pii] 10.1111/j.1742-
875 4658.2009.07432.x
- 876 12. Duschak VG, Cazzulo JJ. Subcellular localization of glutamate dehydrogenases and alanine
877 aminotransferase in epimastigotes of *Trypanosoma cruzi*. *FEMS Microbiol Lett*. 1991;67:
878 131–5. doi:10.1016/0378-1097(91)90343-9
- 879 13. Allmann S, Morand P, Ebikeme C, Gales L, Biran M, Hubert J, et al. Cytosolic NADPH
880 homeostasis in glucose-starved procyclic *Trypanosoma brucei* relies on malic enzyme and
881 the pentose phosphate pathway fed by gluconeogenic flux. *J Biol Chem*. 2013;288: 18494–
882 505. doi:M113.462978 [pii] 10.1074/jbc.M113.462978
- 883 14. Millerioux Y, Morand P, Biran M, Mazet M, Moreau P, Wagnies M, et al. ATP synthesis-
884 coupled and -uncoupled acetate production from acetyl-CoA by the mitochondrial
885 acetate:succinate CoA-transferase and acetyl-CoA thioesterase in *Trypanosoma*. *J Biol*
886 *Chem*. 2012;287: 17186–17197. doi:M112.355404 [pii] 10.1074/jbc.M112.355404
- 887 15. Van Weelden SW, Fast B, Vogt A, Van Der Meer P, Saas J, Van Hellemond JJ, et al.
888 Procyclic *Trypanosoma brucei* do not use Krebs cycle activity for energy generation. *J Biol*
889 *Chem*. 2003;278: 12854–12863.
- 890 16. van Hellemond JJ, Opperdoes FR, Tielens AG. The extraordinary mitochondrion and
891 unusual citric acid cycle in *Trypanosoma brucei*. *Biochem Soc Trans*. 2005;33: 967–71.
- 892 17. Welburn SC, Arnold K, Maudlin I, Gooday GW. *Rickettsia*-like organisms and chitinase
893 production in relation to transmission of trypanosomes by tsetse flies. *Parasitology*.

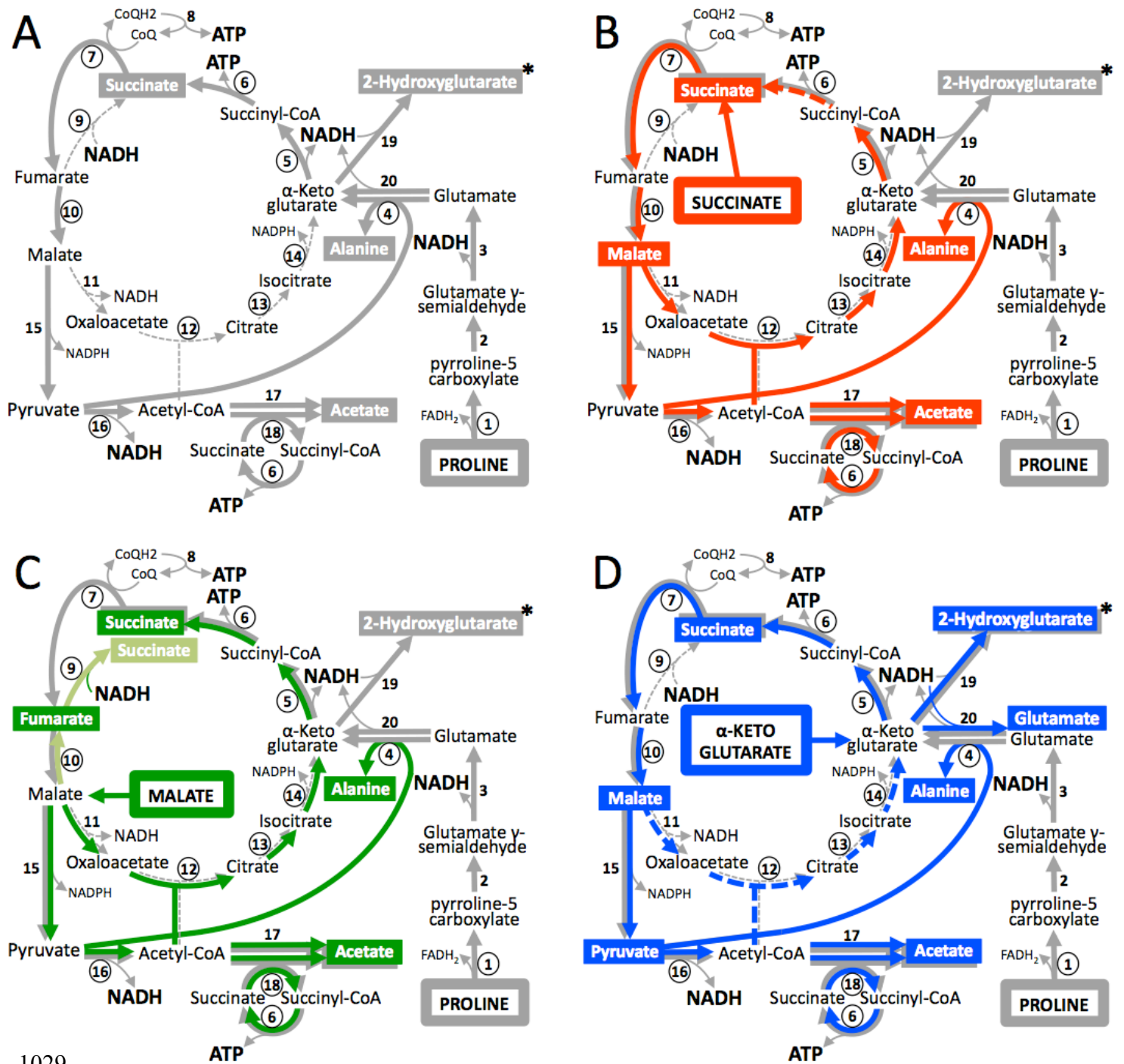
- 894 1993;107 (Pt 2): 141–5. doi:10.1017/s003118200006724x
- 895 18. Hall RJ, Flanagan LA, Bottery MJ, Springthorpe V, Thorpe S, Darby AC, et al. A Tale of
896 Three Species: Adaptation of *Sodalis glossinidius* to Tsetse Biology, *Wigglesworthia*
897 Metabolism, and Host Diet. *MBio*. 2019;10. doi:10.1128/mBio.02106-18
- 898 19. Ong HB, Lee WS, Patterson S, Wyllie S, Fairlamb AH. Homoserine and quorum-sensing
899 acyl homoserine lactones as alternative sources of threonine: a potential role for homoserine
900 kinase in insect-stage *Trypanosoma brucei*. *Mol Microbiol*. 2014;95: 143–156.
901 doi:10.1111/mmi.12853
- 902 20. Balogun RA. Studies on the amino acids of the tsetse fly, *Glossina morsitans*, maintained on
903 in vitro and in vivo feeding systems. *Comp Biochem Physiol Comp Physiol*. 1974;49: 215–
904 22.
- 905 21. Millerioux Y, Ebikeme C, Biran M, Morand P, Bouyssou G, Vincent IM, et al. The
906 threonine degradation pathway of the *Trypanosoma brucei* procyclic form: the main carbon
907 source for lipid biosynthesis is under metabolic control. *Mol Microbiol*. 2013;90: 114–129.
908 doi:10.1111/mmi.12351
- 909 22. Bringaud F, Biran M, Millerioux Y, Wargnies M, Allmann S, Mazet M. Combining reverse
910 genetics and NMR-based metabolomics unravels trypanosome-specific metabolic pathways.
911 *Mol Microbiol*. 2015;96: 917–926. doi:10.1111/mmi.12990
- 912 23. Wargnies M, Bertiaux E, Cahoreau E, Ziebart N, Crouzols A, Morand P, et al.
913 Gluconeogenesis is essential for trypanosome development in the tsetse fly vector. *PLoS*
914 *Pathog*. 2018;14: e1007502. doi:10.1371/journal.ppat.1007502
- 915 24. Coustou V, Besteiro S, Riviere L, Biran M, Biteau N, Franconi JM, et al. A mitochondrial
916 NADH-dependent fumarate reductase involved in the production of succinate excreted by
917 procyclic *Trypanosoma brucei*. *J Biol Chem*. 2005;280: 16559–70.
- 918 25. Coustou V, Biran M, Besteiro S, Riviere L, Baltz T, Franconi JM, et al. Fumarate is an
919 essential intermediary metabolite produced by the procyclic *Trypanosoma brucei*. *J Biol*
920 *Chem*. 2006;281: 26832–46.
- 921 26. Bringaud F, Ebikeme CE, Boshart M. Acetate and succinate production in amoebae,
922 helminths, diplomonads, trichomonads and trypanosomatids: common and diverse metabolic
923 strategies used by parasitic lower eukaryotes. *Parasitology*. 2010;137: 1315–1331.
- 924 27. Muller M, Mentel M, van Hellemond JJ, Henze K, Woehle C, Gould SB, et al. Biochemistry
925 and evolution of anaerobic energy metabolism in eukaryotes. *Microbiol Mol Biol Rev*.
926 2012;76: 444–95. doi:76/2/444 [pii] 10.1128/MMBR.05024-11
- 927 28. Engqvist MK, Esser C, Maier A, Lercher MJ, Maurino VG. Mitochondrial 2-
928 hydroxyglutarate metabolism. *Mitochondrion*. 2014;19 Pt B: 275–81.
929 doi:10.1016/j.mito.2014.02.009
- 930 29. Intlekofer AM, Wang B, Liu H, Shah H, Carmona-Fontaine C, Rustenburg AS, et al. L-2-
931 Hydroxyglutarate production arises from noncanonical enzyme function at acidic pH. *Nat*
932 *Chem Biol*. 2017;13: 494–500. doi:10.1038/nchembio.2307
- 933 30. Johnston K, Kim DH, Kerkhoven EJ, Burchmore R, Barrett MP, Achcar F. Mapping the
934 metabolism of five amino acids in bloodstream form *Trypanosoma brucei* using U-(13)C-
935 labelled substrates and LC-MS. *Biosci Rep*. 2019;39. doi:10.1042/BSR20181601
- 936 31. Bringaud F, Stripecke R, Frech GC, Freedland S, Turck C, Byrne EM, et al. Mitochondrial
937 glutamate dehydrogenase from *Leishmania tarentolae* is a guide RNA-binding protein. *Mol*
938 *Cell Biol*. 1997;17: 3915–23.
- 939 32. Kolev NG, Ramey-Butler K, Cross GA, Ullu E, Tschudi C. Developmental progression to
940 infectivity in *Trypanosoma brucei* triggered by an RNA-binding protein. *Science*. 2012;338:
941 1352–3. doi:338/6112/1352 [pii] 10.1126/science.1229641
- 942 33. Urwyler S, Studer E, Renggli CK, Roditi I. A family of stage-specific alanine-rich proteins
943 on the surface of epimastigote forms of *Trypanosoma brucei*. *Mol Microbiol*. 2007;63: 218–

- 944 228. doi:10.1111/j.1365-2958.2006.05492.x
- 945 34. Dolezelova E, Kunzova M, Dejung M, Levin M, Panicucci B, Regnault C, et al. Cell-based
946 and multi-omics profiling reveals dynamic metabolic repurposing of mitochondria to drive
947 developmental progression of *Trypanosoma brucei*. PLoS Biol. 2020;18: e3000741.
948 doi:10.1371/journal.pbio.3000741
- 949 35. Emmer BT, Daniels MD, Taylor JM, Epting CL, Engman DM. Calflagin inhibition prolongs
950 host survival and suppresses parasitemia in *Trypanosoma brucei* infection. Eukaryot Cell.
951 2010;9: 934–42. doi:10.1128/EC.00086-10
- 952 36. Ryley JF. Studies on the metabolism of protozoa. 9. Comparative metabolism of
953 bloodstream and culture forms of *Trypanosoma rhodesiense*. Biochem J. 1962;85: 211–223.
- 954 37. Vickerman K. Polymorphism and mitochondrial activity in sleeping sickness trypanosomes.
955 Nature. 1965;208: 762–6. doi:10.1038/208762a0
- 956 38. Flynn IW, Bowman IB. The metabolism of carbohydrate by pleomorphic African
957 trypanosomes. Comp Biochem Physiol B. 1973;45: 25–42. doi:10.1016/0305-
958 0491(73)90281-2
- 959 39. Bienen EJ, Maturi RK, Pollakis G, Clarkson AB. Non-cytochrome mediated mitochondrial
960 ATP production in bloodstream form *Trypanosoma brucei brucei*. Eur J Biochem.
961 1993;216: 75–80. doi:10.1111/j.1432-1033.1993.tb18118.x
- 962 40. Dewar CE, MacGregor P, Cooper S, Gould MK, Matthews KR, Savill NJ, et al.
963 Mitochondrial DNA is critical for longevity and metabolism of transmission stage
964 *Trypanosoma brucei*. PLoS Pathog. 2018;14: e1007195. doi:10.1371/journal.ppat.1007195
- 965 41. Wang X, Inaoka DK, Shiba T, Balogun EO, Allmann S, Watanabe YI, et al. Expression,
966 purification, and crystallization of type 1 isocitrate dehydrogenase from *Trypanosoma*
967 *brucei brucei*. Protein Expr Purif. 2017;138: 56–62. doi:10.1016/j.pep.2017.06.011
- 968 42. Riviere L, Moreau P, Allmann S, Hahn M, Biran M, Plazolles N, et al. Acetate produced in
969 the mitochondrion is the essential precursor of lipid biosynthesis in procyclic trypanosomes.
970 Proc Natl Aca Sci USA. 2009;106: 12694–12699.
- 971 43. Forchhammer K, Selim KA. Carbon/Nitrogen Homeostasis Control in Cyanobacteria.
972 FEMS Microbiol Rev. 2019. doi:10.1093/femsre/fuz025
- 973 44. Li F, Xu W, Zhao S. Regulatory roles of metabolites in cell signaling networks. J Genet
974 Genomics. 2013;40: 367–74. doi:10.1016/j.jgg.2013.05.002
- 975 45. Huergo LF, Dixon R. The Emergence of 2-Oxoglutarate as a Master Regulator Metabolite.
976 Microbiol Mol Biol Rev. 2015;79: 419–35. doi:10.1128/MMBR.00038-15
- 977 46. Ryan DG, Murphy MP, Frezza C, Prag HA, Chouchani ET, O'Neill LA, et al. Coupling
978 Krebs cycle metabolites to signalling in immunity and cancer. Nat Metab. 2019;1: 16–33.
979 doi:10.1038/s42255-018-0014-7
- 980 47. Rzem R, Vincent MF, Van Schaftingen E, Veiga-da-Cunha M. L-2-hydroxyglutaric
981 aciduria, a defect of metabolite repair. J Inherit Metab Dis. 2007;30: 681–9.
982 doi:10.1007/s10545-007-0487-0
- 983 48. Girard R, Crispim M, Alencar MB, Silber AM. Uptake of l-Alanine and Its Distinct Roles in
984 the Bioenergetics of *Trypanosoma cruzi*. mSphere. 2018;3.
985 doi:10.1128/mSphereDirect.00338-18
- 986 49. Wolfe AJ. The acetate switch. Microbiol Mol Biol Rev. 2005;69: 12–50.
- 987 50. Ghozlane A, Bringaud F, Souedan H, Dutour I, Jourdan F, Thébault P. Flux analysis of the
988 *Trypanosoma brucei* glycolysis based on a multiobjective-criteria bioinformatic approach.
989 Adv Bioinforma. 2012;2012: 159423.
- 990 51. Brun R, Schonenberger M. Cultivation and in vitro cloning or procyclic culture forms of
991 *Trypanosoma brucei* in a semi-defined medium. Acta Trop. 1979;36: 289–92.
- 992 52. Wirtz E, Leal S, Ochatt C, Cross GA. A tightly regulated inducible expression system for
993 conditional gene knock-outs and dominant-negative genetics in *Trypanosoma brucei*. Mol

- 994 Biochem Parasitol. 1999;99: 89–101.
- 995 53. Wickstead B, Ersfeld K, Gull K. Targeting of a tetracycline-inducible expression system to
996 the transcriptionally silent minichromosomes of *Trypanosoma brucei*. Mol Biochem
997 Parasitol. 2002;125: 211–6.
- 998 54. Bringaud F, Baltz D, Baltz T. Functional and molecular characterization of a glycosomal
999 PPI-dependent enzyme in trypanosomatids: pyruvate, phosphate dikinase. Proc Natl Acad
1000 Sci USA. 1998;95: 7963–8.
- 1001 55. Harlow E, Lane D. Antibodies : a laboratory manual. Cold Spring Harbor Laboratory Press;
1002 1988.
- 1003 56. Sambrook J, Fritsch EF, Maniatis T. Molecular cloning : a laboratory manual. 2nd ed. New
1004 York: Cold Spring Harbor Laboratory Press; 1989.
- 1005 57. Riviere L, van Weelden SW, Glass P, Vegh P, Coustou V, Biran M, et al. Acetyl:succinate
1006 CoA-transferase in procyclic *Trypanosoma brucei*. Gene identification and role in
1007 carbohydrate metabolism. J Biol Chem. 2004;279: 45337–46. doi:10.1074/jbc.M407513200
1008 M407513200 [pii]
- 1009 58. Clayton CE. Import of fructose bisphosphate aldolase into the glycosomes of *Trypanosoma*
1010 *brucei*. J Cell Biol. 1987;105: 2649–54. doi:10.1083/jcb.105.6.2649
- 1011 59. Bringaud F, Peyruchaud S, Baltz D, Giroud C, Simpson L, Baltz T. Molecular
1012 characterization of the mitochondrial heat shock protein 60 gene from *Trypanosoma brucei*.
1013 Mol Biochem Parasitol. 1995;74: 119–23.
- 1014 60. Chaudhuri M, Ajayi W, Hill GC. Biochemical and molecular properties of the *Trypanosoma*
1015 *brucei* alternative oxidase. Mol Biochem Parasitol. 1998;95: 53–68.
- 1016 61. Brown ED, Wood JM. Conformational change and membrane association of the PutA
1017 protein are coincident with reduction of its FAD cofactor by proline. J Biol Chem.
1018 1993;268: 8972–9.
- 1019 62. Bergmeyer HU, Bergmeyer J, Grassi M. Methods of enzymatic analysis. Wiley; 1983.
- 1020 63. Aranda A, Maugeri D, Uttaro AD, Opperdoes F, Cazzulo JJ, Nowicki C. The malate
1021 dehydrogenase isoforms from *Trypanosoma brucei*: subcellular localization and differential
1022 expression in bloodstream and procyclic forms. Int J Parasitol. 2006;36: 295–307.
1023 doi:10.1016/j.ijpara.2005.09.013
1024
- 1025

1026
1027
1028

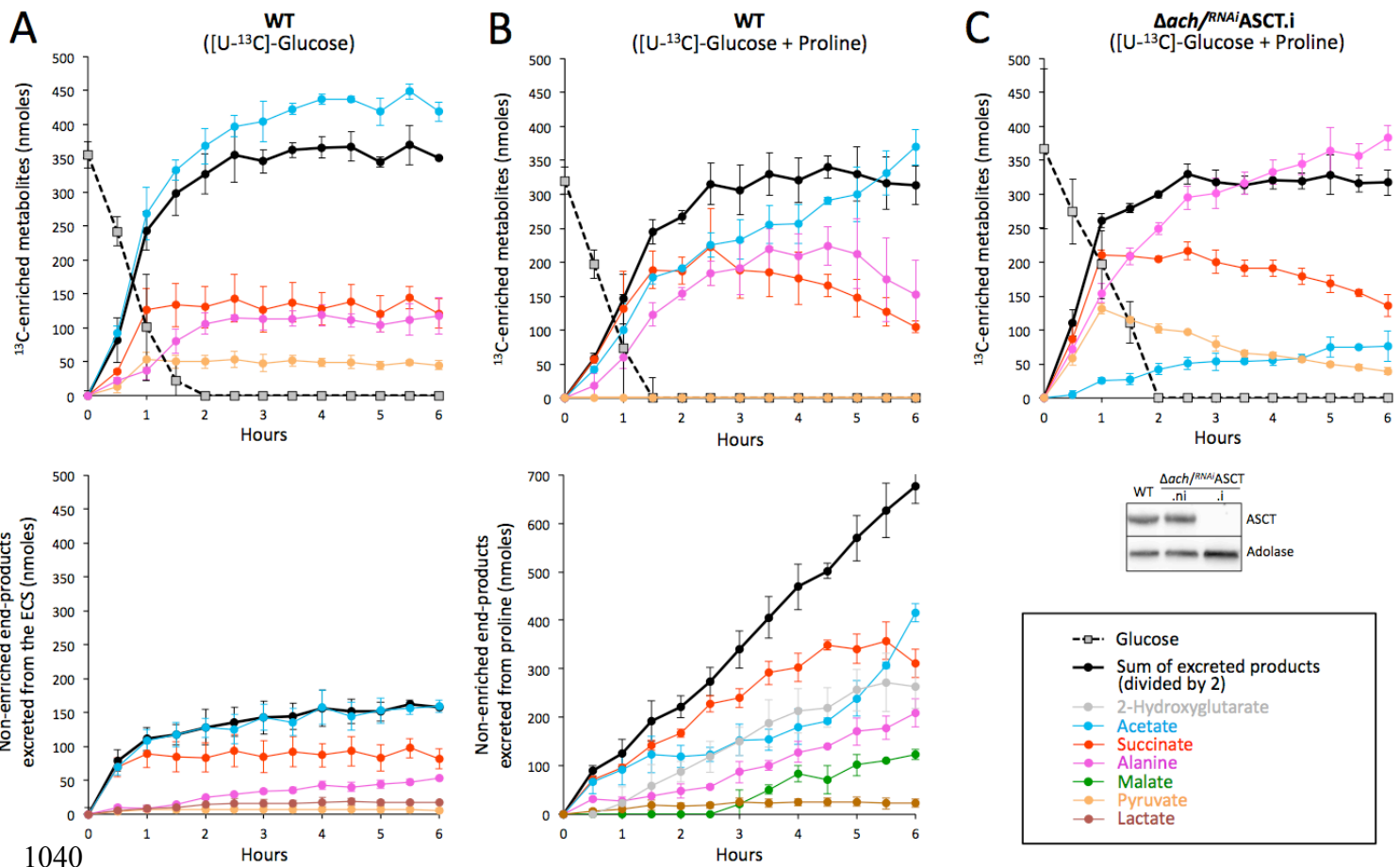
Figure 1



1029
1030

Figure 2

1031
1032
1033
1034
1035
1036
1037
1038
1039

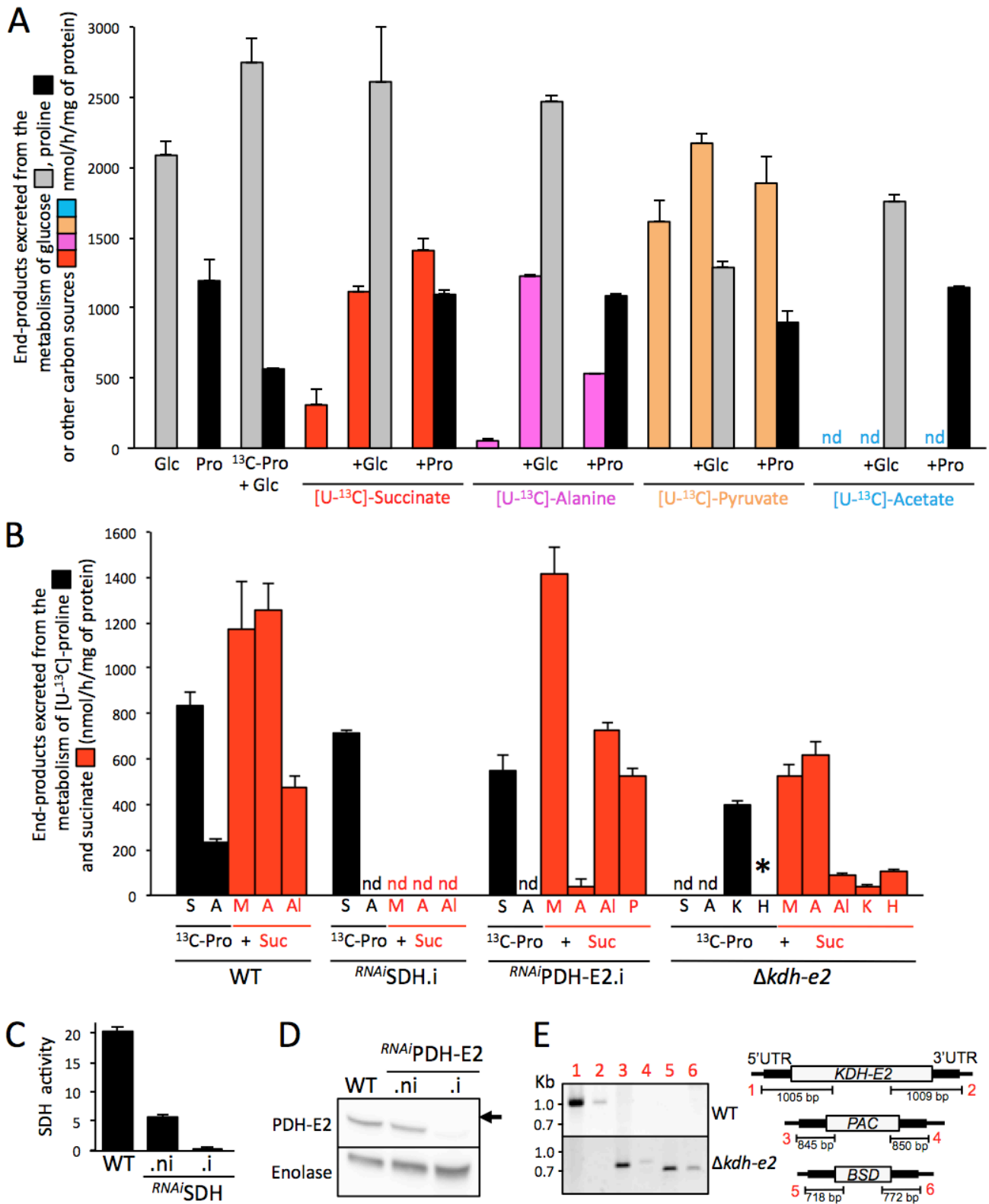


1040

1041

Figure 3

1042

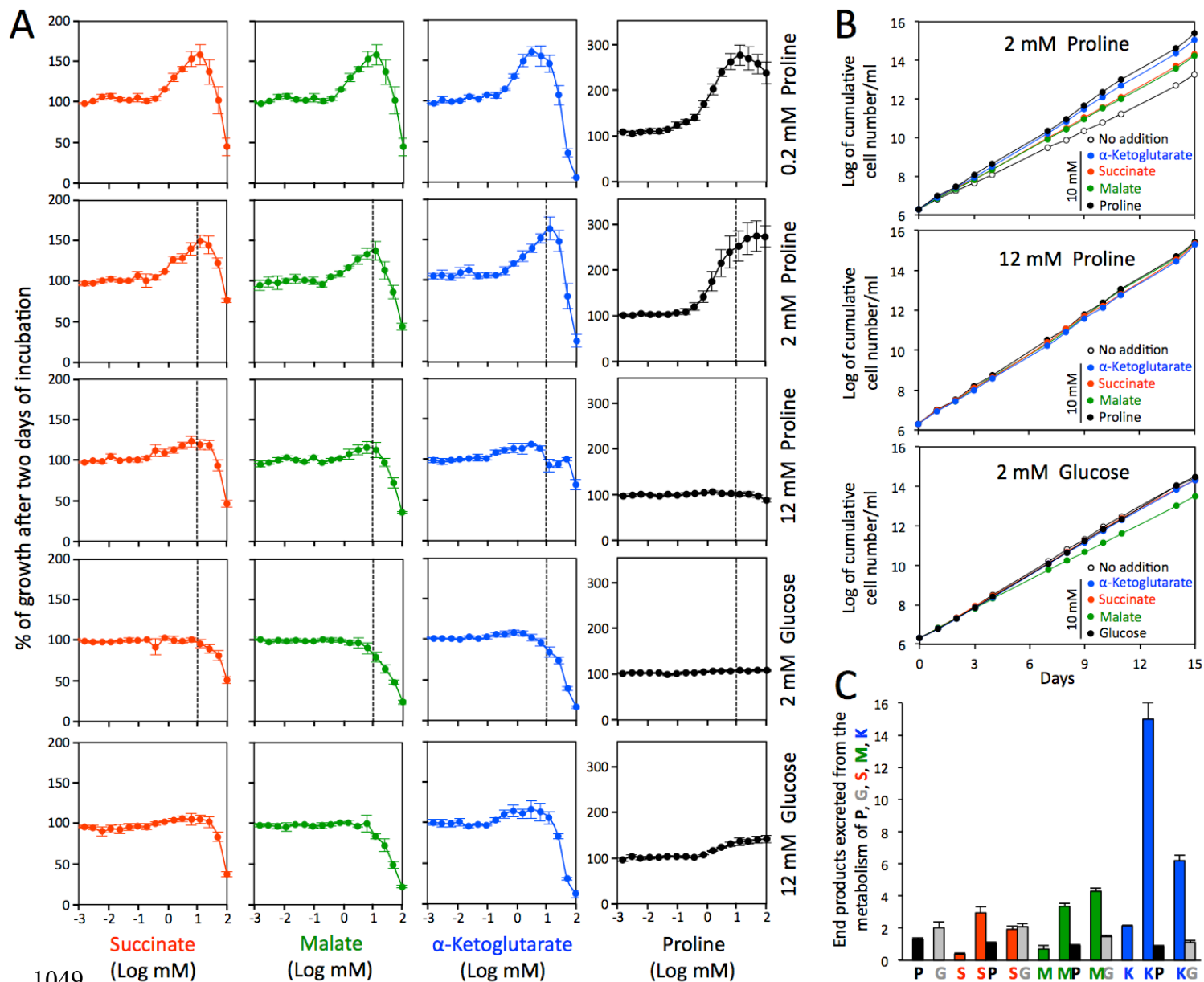


1043

1044

1045
1046
1047
1048

Figure 4

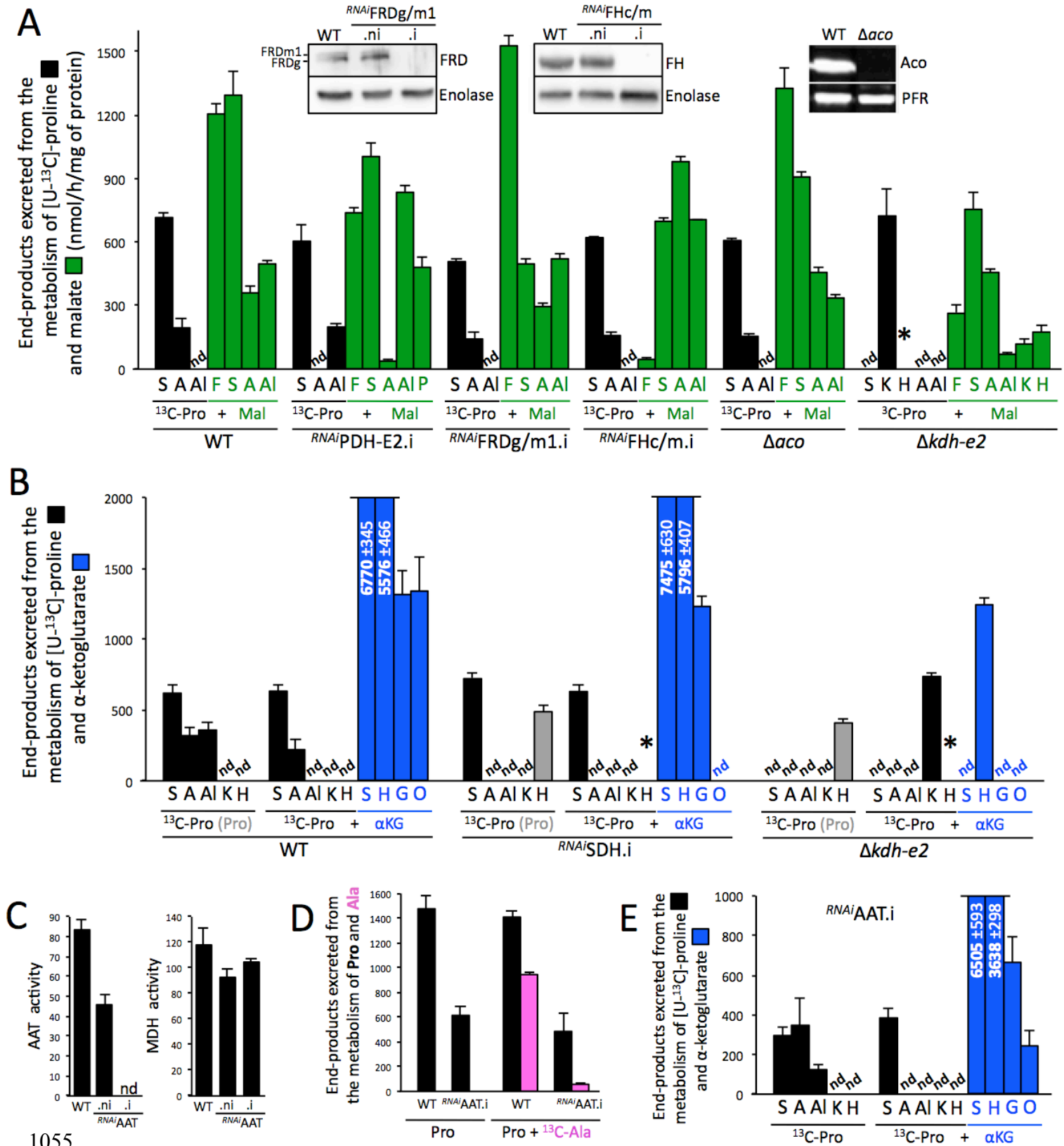


1049
1050
1051
1052

1053

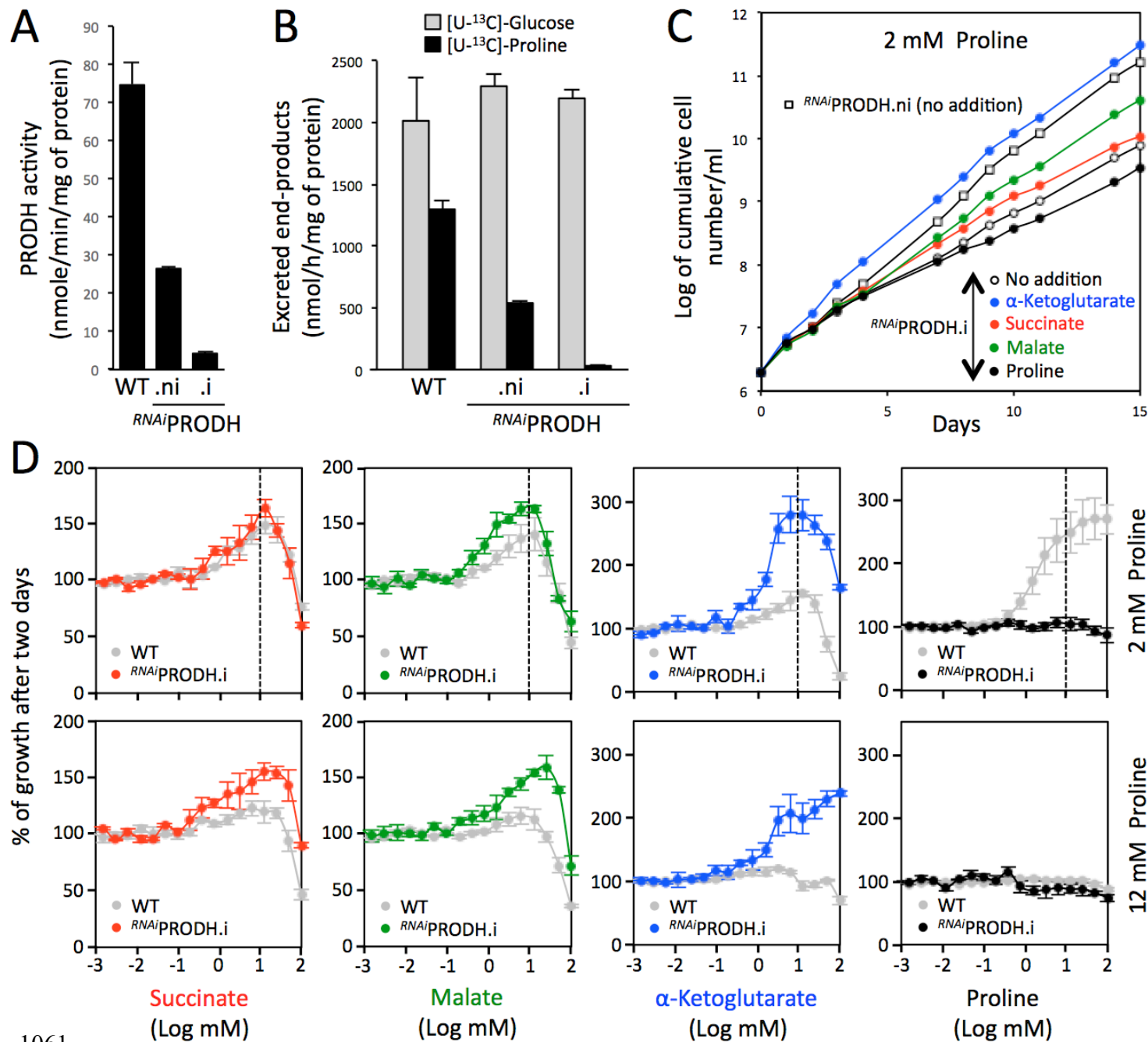
1054

Figure 5



1056
1057
1058
1059
1060

Figure 6

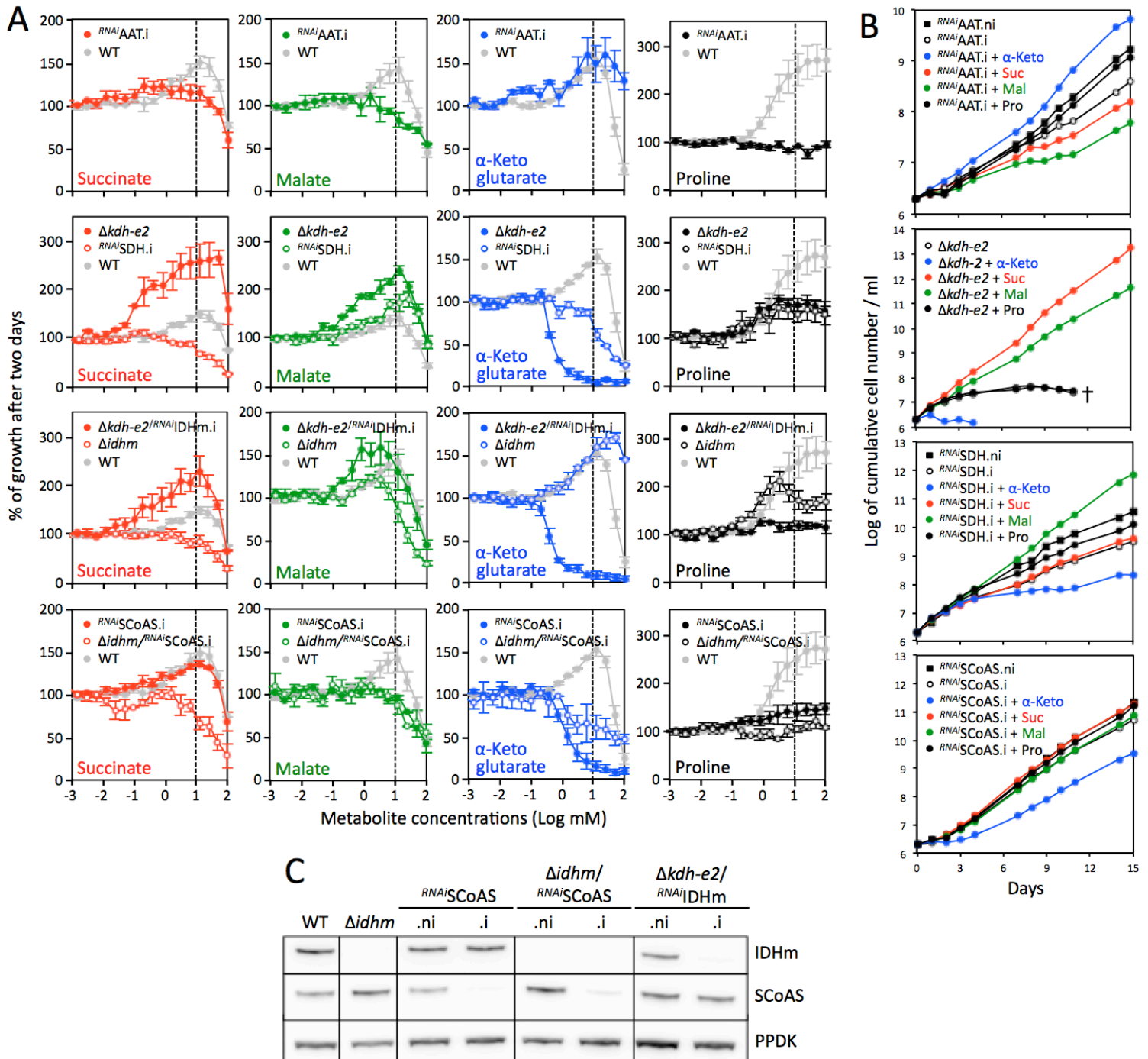


1062

Figure 7

1063

1064



1065

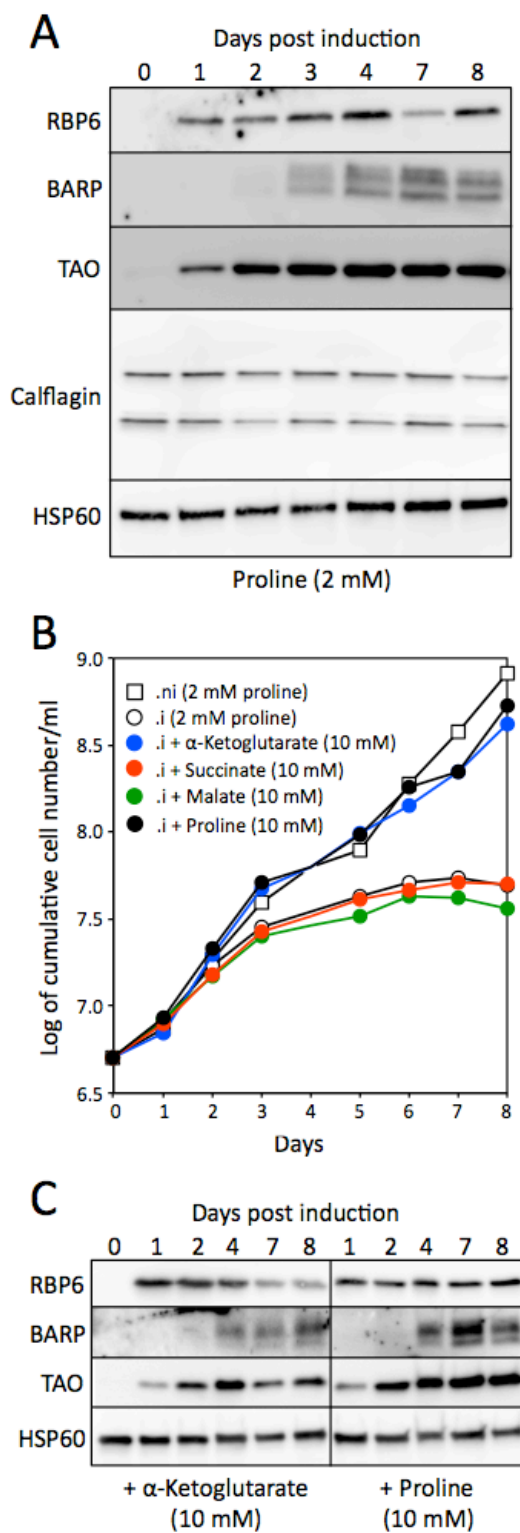
1066

1067

1068

1069
1070
1071

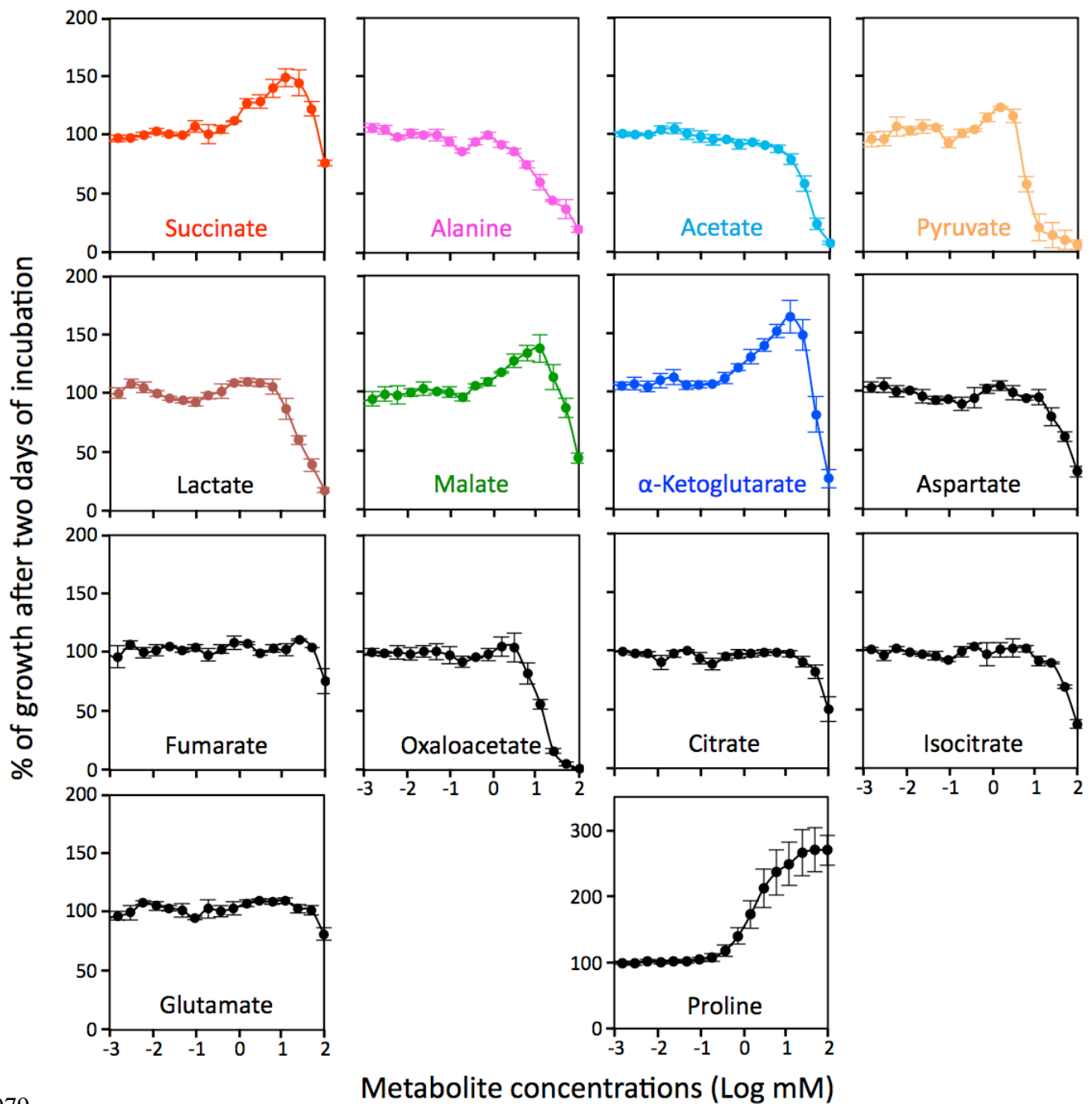
Figure 8



1072

1073 S1 Fig. Growth of the PCF trypanosomes in the glucose-depleted SDM79 medium containing 2
1074 mM proline in the presence of added 10 μ M to 100 mM metabolite, using the Alamar Blue
1075 assay. Incubation was started at 2×10^6 cell density and the Alamar Blue assay was performed
1076 after 48 h at 27°C as described before [23].

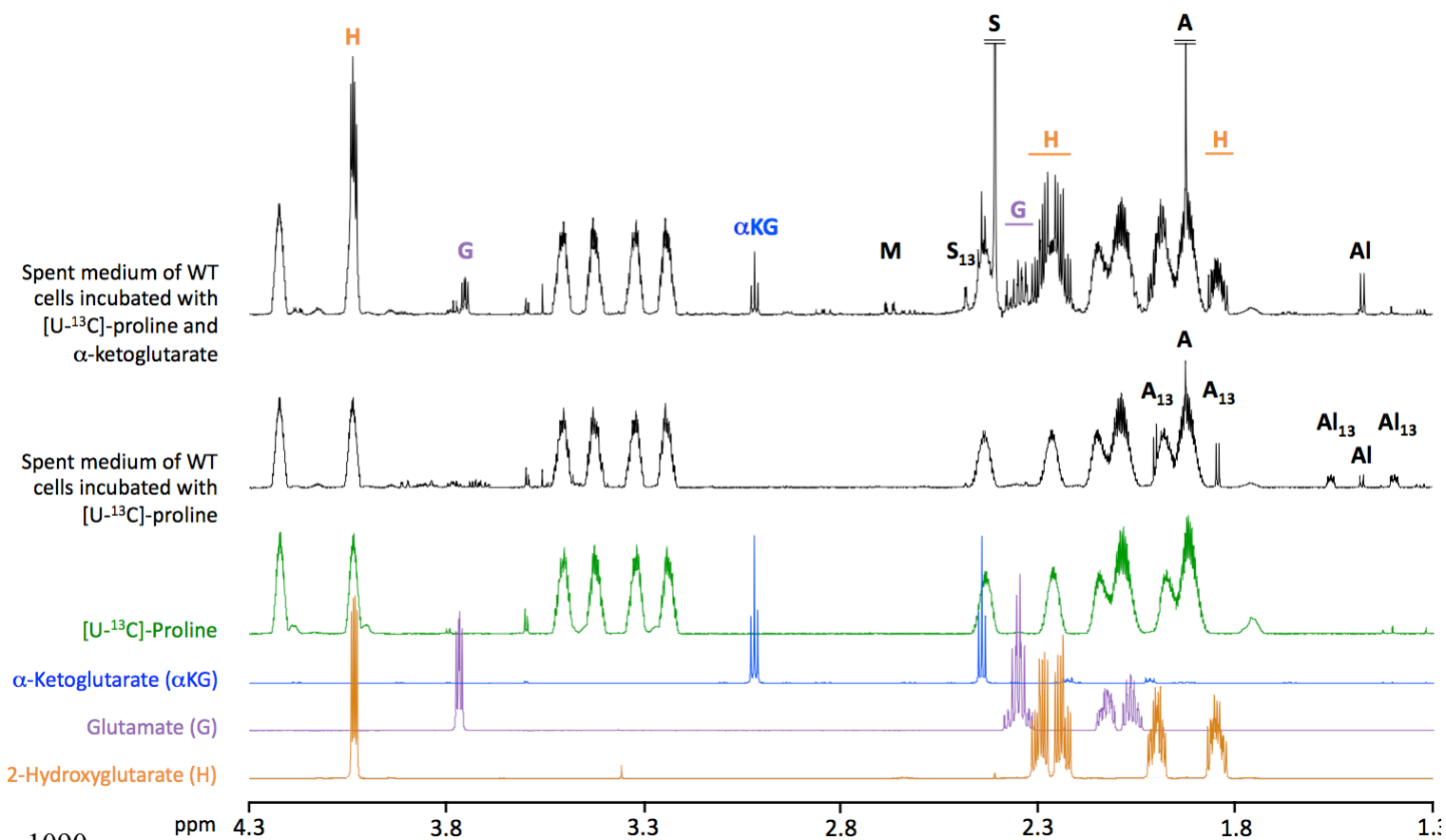
1077
1078



1079
1080

1081 S2 Fig. H-NMR analysis of samples (black) and controls (colored) performed at 800 MHz to
1082 identify acetate (A), alanine (Al), glutamate (G), 2-hydroxyglutarate (H), α -ketoglutarate (α KG),
1083 malate (M), proline and succinate (S). The resonances corresponding to 13 C-enriched molecules
1084 are indicated in index.

1085
1086
1087
1088
1089



1090
1091

1092 S3 Fig. Growth curves of PCF trypanosomes grown in low-proline conditions (0.2 mM) in the
1093 presence or absence of 10 mM proline, glucose, α -ketoglutarate, succinate or malate. Cells were
1094 maintained in the exponential growth phase (between 10^6 and 10^7 cells/ml), and cumulative cell
1095 numbers reflect normalization for dilution during cultivation.

1096

1097

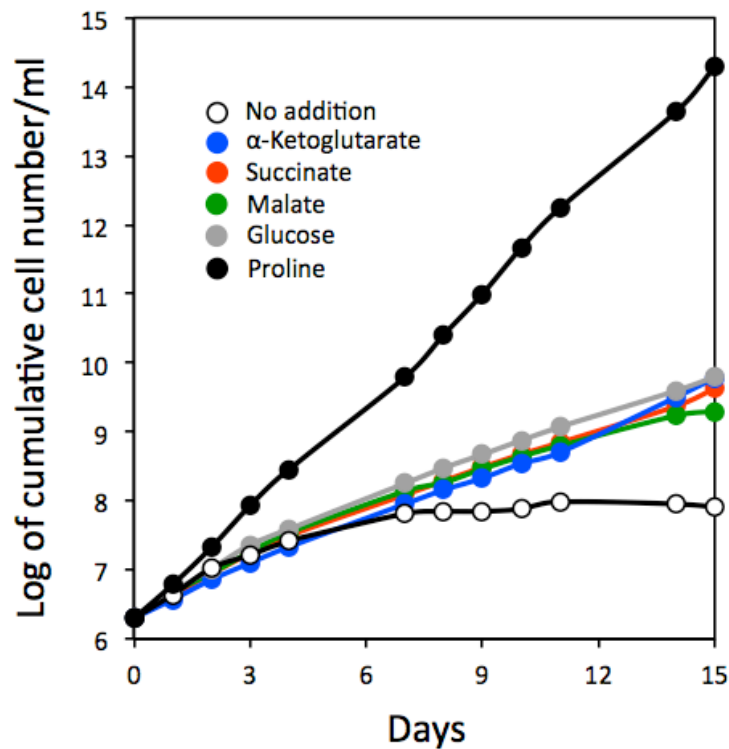
1098

1099

1100

1101

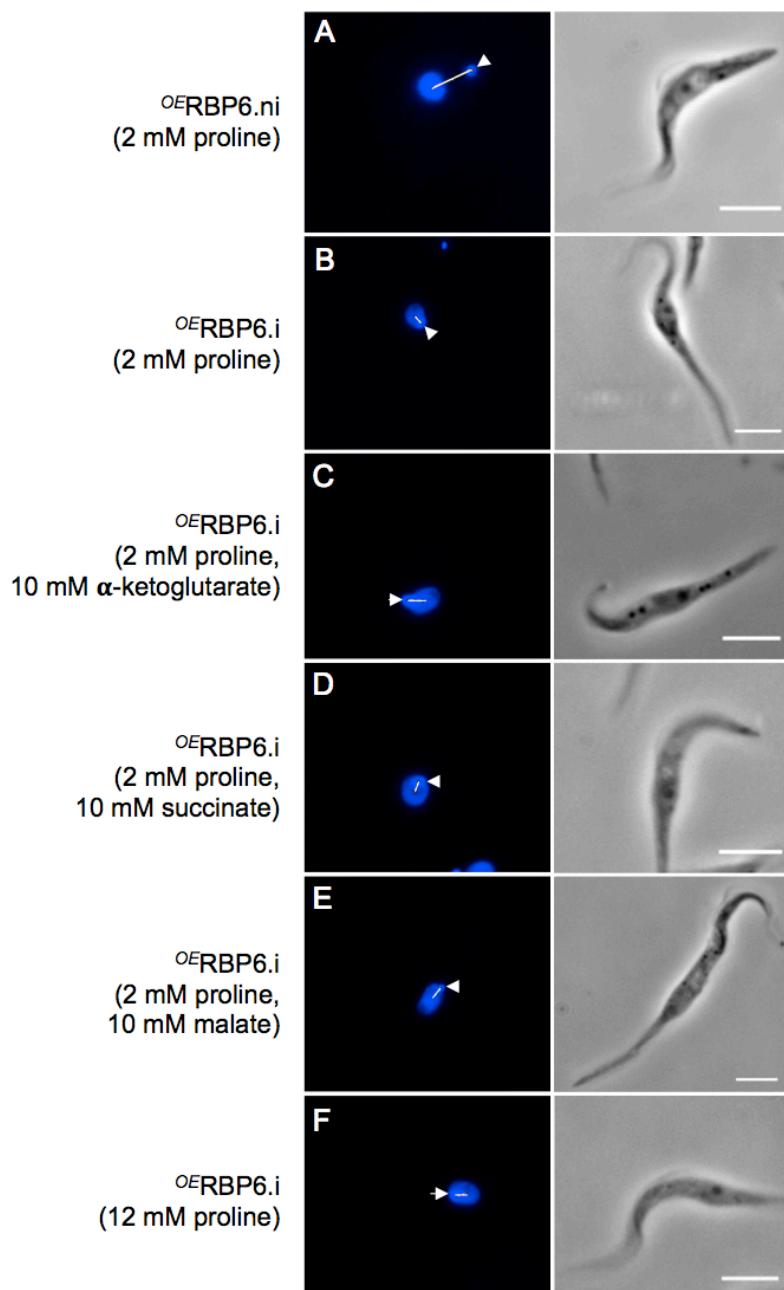
1102



1103 S4 Fig. Imaging of procyclic and epimastigote-like forms. Illustration of microscopic analyses of
1104 non-induced (.ni) (A) or induced (.i) (B-F) $^{OE}RBP6$ cells grown in the presence of 2 mM proline
1105 complemented or not (A-B) with 10 mM of α -ketoglutarate (C), succinate (D), malate (E) or
1106 proline (F). The non-induced population is composed of procyclic trypanosomes (A), while
1107 epimastigote-like cells mainly composed the induced population regardless of the culture
1108 conditions. DAPI staining of DNA is shown on the left panels, in which kinetoplasts are
1109 highlighted by arrowheads and the distance between kinetoplasts and nuclei are shown by white
1110 lines, while the right panels show phase contrast (calibration bar: 5 μ m). These analyses were
1111 performed three days post induction (B-F).

1112

1113



1114 S1 Table. Excreted end-products from the metabolism of carbon sources in the PCF
 1115 trypanosomes. The parasites were incubated with 4 mM [U-¹³C]-succinate, [U-¹³C]-alanine, [U-
 1116 ¹³C]-pyruvate or [U-¹³C]-acetate in the presence or absence of 4 mM glucose or proline.
 1117
 1118

¹³ C-enriched carbon source	/	/	/	Proline	Succinate	Succinate	Succinate	Alanine	Alanine	Alanine	Pyruvate	Pyruvate	Pyruvate	Acetate	Acetate	Acetate
Non-enriched carbon source	ICS ^a	Glucose + ICS	Proline + ICS	Glucose + ICS	ICS	Glucose + ICS	Proline + ICS	ICS	Glucose + ICS	Proline + ICS	ICS	Glucose + ICS	Proline + ICS	ICS	Glucose + ICS	Proline + ICS
Number of samples	6	3	6	3	6	6	6	3	3	3	3	3	3	3	3	3
End products excreted from the metabolism of [carbon sources] (nmoles/hour/10e8 cells)																
Malate [Suc, Ala, Pyr or Ace] ^b					96 ±115	345 ±16	426 ±57	nd	nd	nd	nd	nd	nd	nd	nd	nd
Malate [ICS]	nd ^c	nd		nd	nd			nd			nd	nd	nd	nd	nd	nd
Malate [Glucose and ICS] ^d		nd		nd		188 ±39			98 ±6			nd			68 ±9	
Malate [Proline and ICS] ^e			nd	nd			nd			nd			nd			nd
Fumarate [Suc, Ala, Pyr or Ace]					nd	8 ±3	nd	nd	nd	nd	nd	nd	nd	nd	nd	nd
Fumarate [ICS]	3 ±2				8 ±2			nd			nd	nd	nd	nd	nd	nd
Fumarate [Glucose and ICS]		8 ±4		18 ±2		22 ±2		nd	10 ±2			nd			nd	
Fumarate [Proline and ICS]			7 ±1	nd			11 ±2			nd			4 ±2			1 ±1
Hydroxyglutarate [Suc, Ala, Pyr or Ace]					nd	nd	nd	nd	nd	nd	nd	nd	nd	nd	nd	nd
Hydroxyglutarate [ICS]	nd				nd			nd			nd	nd	nd	nd	nd	nd
Hydroxyglutarate [Glucose and ICS]		nd		nd				nd			nd	nd			nd	
Hydroxyglutarate [Proline and ICS]			205 ±11	nd			194 ±14			326 ±11			212 ±20			196 ±4
Succinate [Suc, Ala, Pyr or Ace]					nd	nd	nd	54 ±15	101 ±1		nd	170 ±12	nd	nd	nd	nd
Succinate [ICS]	23 ±12				210 ±12			31 ±7			27 ±1			30 ±3		
Succinate [Glucose and ICS]		288 ±15		390 ±9		1009 ±188			191 ±3			113 ±4			237 ±8	
Succinate [Proline and ICS]			186 ±36	185 ±4*			820 ±34			269 ±6			130 ±6			166 ±1
Pyruvate [Suc, Ala, Pyr or Ace]					nd	nd	nd	nd	118 ±1		nd	nd	nd	nd	nd	nd
Pyruvate [ICS]	nd				nd			nd			113 ±6	nd	nd	nd	nd	nd
Pyruvate [Glucose and ICS]		40 ±2		nd					34 ±2			584 ±19			109 ±4	
Pyruvate [Proline and ICS]			nd	nd						nd			nd			nd
Acetate [Suc, Ala, Pyr or Ace]					158 ±5	762 ±35	726 ±78	nd	1006 ±23	532 ±4	182 ±7	760 ±17	240 ±31	nd	nd	nd
Acetate [ICS]	88 ±16				102 ±4			20 ±6			90 ±4			161 ±4		
Acetate [Glucose and ICS]		1728 ±81		2015 ±171		1350 ±144			332 ±7			678 ±18			1411 ±33	
Acetate [Proline and ICS]			580 ±82	335 ±8*			191 ±13			119 ±3			385 ±29			479 ±5
Alanine [Suc, Ala, Pyr or Ace]					55 ±5	nd	255 ±34	nd			1021 ±45	1033 ±34	1227 ±60	nd	nd	nd
Alanine [ICS]	65 ±9				31 ±5			205 ±53			nd			57 ±3		
Alanine [Glucose and ICS]		22 ±1		323 ±8		23 ±5			2080 ±28			56 ±2			44 ±3	
Alanine [Proline and ICS]			223 ±34	44 ±2*			46 ±9			532 ±9			242 ±27			303 ±6
Lactate [Suc, Ala, Pyr or Ace]					nd	nd	nd	nd	nd	nd	230 ±104	208 ±12	420 ±111	nd	nd	nd
Lactate [ICS]	nd				14 ±15			nd			nd		nd	nd	nd	nd
Lactate [Glucose and ICS]		nd		nd		16 ±18										
Lactate [Proline and ICS]			nd	nd			9 ±10			nd			nd			nd
Total [Suc, Ala, Pyr or Ace]					309 ±115	1115 ±38	1408 ±83	54 ±15	1226 ±25	532 ±4	1613 ±147	2171 ±71	1887 ±187	nd	nd	nd
Total [ICS]	179 ±23				365 ±28			256 ±66			224 ±8			248 ±7		
Total [Glucose and ICS]		2085 ±94		2746 ±169		2608 ±392			2734 ±36			1430 ±39			1800 ±47	
Total [Proline and ICS]			1193 ±148	565 ±9*			1261 ±34			1245 ±19			972 ±83			1145 ±14

1120

1121

1122 ^a ICS (internal carbon source): intracellular carbon source of unknown origin metabolized by the
 1123 PCF trypanosomes

1124 ^b Amounts of end-products excreted (here malate) from the carbon source indicated in brackets,
 1125 expressed as nmoles excreted per h and per 10⁸ cells.

1126 ^c nd: not detectable

1127 ^d End-products excreted (here malate) from glucose or the ICS, which are both non-enriched

1128 ^e End-products excreted (here malate) from proline or the ICS, which are both non-enriched. The
 1129 asterisks mean that in this particular experiment the values correspond to proline only, since
 1130 it is ¹³C-enriched.

1131

1132